ADDIS ABABA UNIVERSITY

ADDIS ABABA INSTITUTE OF TECHNOLOGY

SCHOOL OF MULTIDISCIPLINARY ENGINEERING

CENTER FOR MATERIALS ENGINEERING

MASTER THESIS

Investigation of Electrical and Optical Properties of Cadmium Sulfide doped with Selenium Using Density Functional Theory

By: Wari Girmaye Deye /GSR/5147/15

A Thesis Submitted to the Center for Materials Engineering in Partial Fulfillment of the Requirements for the Master's Degree of Science in Materials Engineering

Feb, 2025

Ethiopia

This attests to the fact that the thesis named "Investigation of Electrical and optical properties of Cadmium Sulfide doped with Selenium Using Density Functional Theory." is written and prepared by Wari Girmaye Deye in partial compliance with the specifications of the degree of Master of Science in Materials Engineering.

Approval by the Board of Examiners

	Signature	Date
Georgies Alene (PhD)		04/02/2025
Advisor		
Kingsly Obodo(PhD)		
Co. Advisor		
Antaneh Wodaje (PhD)		05/02/2025
Internal Examiner		
Aman Kassaye (PhD)		04/02/2025
External Examiner		
Eng. Antaneh Marelign (PhD)		04/02/2025
Chairman		

i

DECLARATION

I so affirm that the research being presented in this thesis, which is termed "Investigation of Electrical and Optical Properties of Cadmium Sulfide doped with Selenium Using Density Functional Theory." is original work of mine that hasn't been submitted for credit towards a degree from another university. As a result, I've given due credit to all of the sources I utilized to create this thesis.

	signature	Date
Name: Wari Girmaye Deye	WG	04/02/2025

ii

ACKNOWLEDGMENT

I want to begin by thanking my Lord and Savior JESUS CHRIST for making it possible to complete my master's degree. After that, I would like to express my gratitude to Dr. Georgies Alene, my adviser, for his guidance, inspiration, and persistent support during the completion of my MSc thesis. Apart from my mentor, I want to thank Dr. Kingsley Obodo for his invaluable resources, without which I could not have completed my thesis. In closing, I would like to thank my family and friends for their invaluable support in helping me finish my thesis.

ABSTRACT

In this work, density functional theory is used to study the effect of selenium doping on the electrical and optical characteristics of CdS. The wurtzite structure of CdS were modeled and doped with 1.85%, 6.25%, 12.5% and 25% quantities of Se atoms. For the pristine CdS and doped CdS systems, the electronic band structure, density of states, optical absorption, optical reflectivity, loss function, optical conductivity, dielectric function, and refractive index were computed. An increase in Se concentration is observed to cause a reduction in the band gap of CdS and a shift in the optical absorption edge. Moreover, the presence of Se dopants also modifies the optical absorption, optical reflectivity, loss function, optical conductivity, dielectric function, and refractive index. The optical properties for Al doped CdS has improved between 0eV to 5eV.For Zn doped CdS the optical properties are improved between 4eV to 6eV. For Na doped CdS the optical properties are improved except absorption and conductivity. For this research optical absorption is improved at 8eV to 10eV, optical reflectivity is improved at 8eV to 10eV, conductivity is improved at 6eV to 8eV, dielectric function is improved at 3eV to 4eV and refractive index is improved at 3 to 4eV. These results shed important light on how Se doping affects the functionality of CdS-based optoelectronic systems.

***Keywords**: Cadmium sulfide, Wurtzite, Selenium doping, Density functional theory, Electronic properties, Optical properties*

TABLE OF CONTENTS

LIST OF FIGURES

LIST OF TABLES

LIST OF ACRONYMS

CBD	Chemical Vapor Deposition
CdS	Cadmium Sulfide
CIF	Crystallographic Information File
COD	Crystallographic Open Database
CVD	Chemical Bath Deposition
DFT	Density Functional Theory
FCC	Face Centered Cubic
GGA	Generalized Gradient Approximation
LED	Light Emitting Diodes
MBE	Molecular Beam Epitaxy
NEB	Nudged Elastic Band
PBE	Perdew-Burke-Ernzerhof
PDOS	Partial Density of States
PP	Pseudo Potentials
PW	Plane Waves
QE	Quantum ESPRESSO
QM	Quantum-Mechanics
Se	Selenium
SEM	Scanning Electron Microscope
Te	Tellurium
TDOS	Total Density of States
PDOS	Partial Density of States

CHAPTER ONE

1. Introduction

Large band gap semiconductors of the II–VI class have a wide range of potential uses such as solar cells, photovoltaic and optoelectronic devices. A technological push was identified in this field of study through research based on theoretical and experimental analysis. [1] II-VI semiconductor cadmium sulfide (CdS) has significant uses in energy applications. It is a direct band gap n-type semiconductor that finds extensive use in electronic instruments, making it highly significant technologically. It serves as heterojunction solar cell window material. Light emitting diodes, photo detectors, Sensors, address decoders, and electrically driven lasers are a few fields in which it finds use.[2] Other extended applications of CdS that make its usage for production include nonlinear optics, electroluminescent displays, photoconductors, and bio-sensing devices. [3]

Rocksalt, Wurtzite, and zinc mix are examples of naturally occurring CdS structural formations. Wurtzite and zinc mix formations are both discovered to be energetically degenerate and polymorphous. The second structure is more stable and symmetrically hexagonal with four atomic bases, whereas the first structure is a face-centered cubic (FCC) lattice with diatomic foundation. While rocksalt shapes (cubic) may be seen in nanocrystallite form, wurtzite structures can be seen in both bulk and nanocrystallite forms. Additionally, at high pressures of around 2.5–3.5 GPa, the rocksalt phase is found [4].

The study of CdS is important for forecasting electronic characteristics through theoretical and experimental approaches. The optical, electronic, magnetic, electrical, and piezoelectric characteristics of CdS may be improved by doping it with certain dopants [5]. Many investigations have been carried out recently to look at the optical, electrical, and related characteristics utilizing both theoretical and experimental techniques. Theoretical and experimental scientists continue to be interested in CdS because to its remarkable and rational qualities, which include low cost, high efficiency, and improved optoelectronic capabilities. [6]

Cadmium sulfide's (CdS) semiconductor qualities are greatly improved by selenium doping. It improves electrical conductivity, which is necessary for solar cells and photodetectors, by raising carrier concentration. Selenium allows for fine control over electrical properties by acting as either an n-type or p-type dopant. It also alters the band gap, allowing for adjustable optical characteristics that are essential for solar cells and light-emitting diodes (LEDs). Efficiency is increased in selenium-doped CdS, especially in thin-film solar cells, due to improved light absorption and decreased recombination losses. All things considered, selenium doping maximizes CdS, increasing its uses and improving the functionality of different technologies.

Many experimental investigations have been conducted to investigate the physical characteristics of doped CdS, but a few theoretical study notes have been published [7] to support experimental predictions. The topic of doping CdS with transition metals has been studied for many years.

For Zn doped CdS the optical properties are improved between the range of 4eV to 6eV. For Al doped CdS the optical properties are improved in the range 0eV to 6eV. For Na doped CdS optical absorption and optical conductivity didn’t improve but the remaining optical properties like reflectivity, refractive index and dielectric function are improved with the introduction of the dopant.

In the current work, computational analysis was used to examine electrical and optical characteristics of the Se doped Wurtzite CdS system by replacing the S atoms with Se atoms. The investigated properties include band structure, optical absorption, conductivity, index of refraction, Loss Function, reflectivity, and dielectric constant. The total density of states (TDOS) were also computed. The study has examined a number of surprising facts regarding the optical characteristics of the CdS: Se combination. These facts include band gap reduction and improved optical properties.

1.1 BACKGROUND

Cadmium sulfide (CdS), a well-known material in the II-VI semiconductor family, has been widely studied and utilized in various optoelectronic applications, [8] such as light-emitting diodes (LEDs), solar cells, and photodetectors. Its direct bandgap of approximately 2.4 eV makes CdS particularly suitable for both emitting and absorbing light in the visible spectrum. This

characteristic allows CdS to perform effectively in devices that require efficient light interaction. Furthermore, the electrical and optical properties of CdS can be significantly enhanced through the process of doping, where specific impurities are introduced into the material. By carefully selecting these dopants, researchers can tailor the performance of CdS-based devices to meet the demands of various applications, improving their efficiency and functionality. This adaptability not only broadens the potential uses of CdS in advanced technologies but also positions it as a key material in the development of next-generation optoelectronic devices. Overall, the combination of CdS's inherent properties and the benefits derived from doping makes it a versatile and valuable component in the field of materials science and engineering.[9]

Doping cadmium sulfide (CdS) presents a promising approach to enhance its performance in various applications. As a Group VI element, selenium can effectively substitute sulfur (S) within the CdS lattice. [10] This substitution can significantly impact the material's overall performance, charge transport capabilities, and electronic structure. Specifically, the incorporation of Se atoms has the potential to modify key properties of CdS, including its bandgap, carrier concentration, and mobility. These characteristics are crucial for optimizing the functionality of CdS in a wide range of optoelectronic devices, such as solar cells,[11] light-emitting diodes (LEDs), and photodetectors. By adjusting the concentration of selenium doping, researchers can tailor these properties to achieve desired performance metrics, ultimately leading to more efficient and effective devices. This ability to fine-tune the material's characteristics through doping not only enhances the utility of CdS in existing applications but also opens avenues for developing new technologies that leverage its improved capabilities. Thus, selenium doping represents a valuable strategy for advancing the performance of CdS-based optoelectronic materials.

Density Functional Theory (DFT) serves as a powerful computational tool for analyzing the structural, electrical, and optical properties of semiconductor materials,[12] including cadmium sulfide (CdS) and its selenium-doped variants (CdS:Se). By leveraging DFT simulations, researchers can gain fundamental insights into the underlying mechanisms that influence how selenium doping affects the electrical characteristics of CdS. This understanding is crucial for the logical design and optimization of CdS-based devices, as it allows scientists to predict how changes in doping concentration and configuration can impact the material's performance.

Through DFT, it is possible to explore various aspects of systems, such as changes in the electronic band structure and optical properties. [13] These simulations provide a detailed picture of how Se atoms interact with the CdS lattice and alter its electronic properties, such as bandgap energy and carrier mobility. This information is vital for tailoring CdS for specific applications in optoelectronics, including solar cells, light-emitting diodes (LEDs), and photodetectors. [14].

Moreover, DFT can facilitate the identification of optimal doping levels and configurations that maximize the efficiency of CdS-based devices. By simulating different scenarios, researchers can systematically investigate the effects of various doping strategies, leading to informed decision-making in material development. Overall, DFT not only enhances our understanding of the fundamental properties of CdS and CdS:Se systems but also plays an essential role in advancing the design and optimization of next-generation semiconductor devices.

1.2 Statement of the Problem

Cadmium sulfide (CdS) is a semiconductor with significant applications in photovoltaics [15], photocatalysis, and optoelectronics due to its favorable electrical and optical properties. Doping CdS has emerged as a promising approach to enhance these properties, potentially leading to improved performance in various technologies. [16] Density Functional Theory (DFT) provides a robust computational framework to investigate the electronic structures and properties of semiconductor materials, allowing for an in-depth understanding of how doping affects their characteristics.

Despite the potential benefits of CdS, a significant knowledge gap exists regarding how varying concentrations of selenium influence the material's electrical and optical properties. This limited understanding poses challenges in optimizing CdS-based devices, such as solar cells and photodetectors, which rely on these critical properties for enhanced performance. Without comprehensive insights into the relationship between selenium doping levels and the resulting material characteristics, researchers and engineers may struggle to tailor CdS for specific applications, leading to suboptimal device efficiency. Consequently, this hampers the development of advanced technologies that could benefit from improved semiconductor performance. As the demand for efficient renewable energy solutions continues to grow, addressing this knowledge gap becomes increasingly urgent. A deeper understanding of how selenium concentrations affect the

fundamental properties of CdS is essential for guiding the design and fabrication of more effective devices. By bridging this gap, we can unlock the full potential of Se-doped CdS, ultimately contributing to more sustainable and efficient technologies in the fields of energy and electronics.

The lack of comprehensive insights into the electrical and optical properties of Se-doped CdS affects the development of more efficient solar cells, sensors, and other electronic devices. This inefficiency may lead to higher production costs and slower advancements in renewable energy technologies, ultimately hindering progress toward sustainable energy solutions.

The primary individuals affected by this knowledge gap include researchers and engineers in the fields of materials science, renewable energy, and semiconductor technology, as well as industries that rely on CdS for the development of advanced electronic components. Additionally, broader societal impacts include the potential delays in the transition to more sustainable energy solutions, affecting communities' dependent on renewable energy technologies.

Current literature lacks detailed computational studies that systematically explore the relationship between selenium doping levels and the resultant electrical and optical properties of CdS. While some studies have addressed related aspects, [17] they often overlook critical parameters such as the concentration-dependent effects and their implications on the performance of CdS-based devices.

The primary objective of this research is to investigate the effects of varying selenium doping concentrations on the electrical and optical properties of cadmium sulfide (CdS) using Density Functional Theory (DFT) simulations. By systematically analyzing how different levels of selenium doping influence these properties, the study aims to provide valuable insights that can inform the design of more efficient semiconductor devices. Understanding the relationship between doping concentrations and the resulting material characteristics will enhance the performance of CdS in applications such as photovoltaics and optoelectronics, ultimately and improved electronic components.

1.3 Objectives of the study

1.3.1 General Objective

- To computationally analyze the effects of Selenium doping on the electrical and optical properties of Cadmium Sulfide using Density Functional Theory Simulations.

1.3.2 Specific Objectives

- To determine how Selenium doping alters the electronic properties of CdS, including its band gap, total density of states(TDOS) and band structure using DFT simulations.
- To evaluate the impact of selenium concentration on key optical properties (optical absorption, optical reflectivity, loss function, optical conductivity, dielectric function, and refractive index) using DFT simulations.
- To compare computational findings with experimental studies to validate the trends observed and discuss the implications for optoelectronic applications.

1.4 Scope of the Study

The material system under investigation in this study comprises CdS doped with Se, a semiconductor known for its favorable electronic and optical properties. CdS is a II-VI compound semiconductor that exhibits a wide bandgap, making it suitable for applications in photovoltaics and optoelectronics. Doping CdS with selenium introduces new energy levels within the band structure, influencing both electrical conductivity and optical absorption characteristics. By systematically varying the concentration of selenium, this research aims to elucidate its effects on the electronic properties of CdS. DFT simulations will be utilized to model the interactions and assess how different Se doping levels alter the material's electronic structure. This investigation not only seeks to enhance the understanding of CdS:Se as a material system but also aims to optimize its properties for improved performance in various technological applications, particularly in renewable energy devices.

The computational methodology for investigating the electrical and optical properties of CdS doped with Se employs DFT as the primary theoretical framework. First, the crystal structure of CdS will be modeled, incorporating varying concentrations of selenium to analyze its doping effects. The generalized gradient approximation (GGA) will be used to account for exchange-correlation effects, ensuring accurate predictions of the electronic properties. DFT calculations will include optimizing the geometric structure and evaluating the band structure, density of states, and optical properties. The simulations will be conducted using well-established quantum espresso

software, which allows for precise calculations of the electronic interactions within the material. By systematically varying the selenium concentration, this methodology aims to provide comprehensive insights into how doping influences the electrical and optical properties of CdS, ultimately aiding in the design of more efficient semiconductor devices.

The electronic structure analysis of cadmium sulfide (CdS) doped with selenium (Se) will focus on understanding how varying concentrations of Se influence the material's electronic properties. Utilizing DFT, the study will calculate the band structure and total DOS for different doping levels. This analysis will reveal shifts in the conduction and valence bands, as well as the introduction of mid-gap states that can enhance electrical conductivity. By comparing the electronic structures of pure CdS and Se-doped CdS, we can identify the impact of selenium on bandgap narrowing and the overall electronic behavior of the material. This comprehensive electronic structure analysis will provide essential insights into the relationship between doping concentration and the resultant electrical properties, guiding future advancements in semiconductor technology.

The broader implications of investigating the electrical and optical properties of CdS doped with Se extend beyond fundamental science to significant technological advancements. By enhancing our understanding of how Se doping affects CdS, this research can lead to the development of more efficient semiconductor devices, particularly in renewable energy applications such as solar cells and photodetectors. Improved electrical and optical property can directly enhance the performance of these devices, making them more competitive and cost-effective. Additionally, insights gained from this study may inform the design of novel materials with tailored properties for specific applications, contributing to innovations in electronics and optoelectronics. As the demand for sustainable energy solutions grows, optimizing CdS-based materials will play a crucial role in advancing clean energy technologies. Ultimately, this research has the potential to foster significant progress in both the scientific community and the broader field of renewable energy.

1.5 Significance of the study

The scientific contribution of this investigation into the electrical and optical properties of CdS doped with Se lies in its novel application of DFT to systematically explore the effects of varying selenium concentrations on material characteristics. This study will provide valuable insights into the electronic structure and fundamental behavior of Se-doped CdS, filling a critical knowledge gap in semiconductor research. By elucidating the relationship between doping levels and

electrical conductivity, as well as optical absorption properties, the findings will contribute to a deeper understanding of how to optimize CdS for enhanced performance in practical applications. Additionally, the research will establish a theoretical framework that can be applied to other semiconductor materials, promoting further exploration of doping mechanisms and their effects. Ultimately, this work aims to advance both the theoretical basis and practical applications of CdS-based materials, facilitating the development of more efficient and sustainable technologies in the field of electronics and renewable energy.

The technological implications of investigating the electrical and optical properties of CdS doped with Se are significant for advancing semiconductor applications. By understanding how selenium doping influences the electronic and optical characteristics of CdS, this research can lead to the development of more efficient solar cells and photodetectors, critical components in renewable energy systems and optoelectronic devices. Enhanced electrical conductivity and tailored optical absorption properties can improve the efficiency and performance of these devices, making them more viable for commercial applications. Furthermore, the insights gained may guide the design of new materials that leverage similar doping strategies, fostering innovation in the semiconductor industry. As global energy demands shift towards sustainable solutions, optimizing CdS-based materials through targeted doping could play a pivotal role in the advancement of clean energy technologies, ultimately contributing to a more sustainable future.

The investigation of electrical and optical properties of CdS doped with Se represents a significant advancement in computational materials science by demonstrating the power of DFT in predicting and analyzing complex material behaviors. This research not only showcases the ability of DFT to provide detailed insights into the electronic structure and properties of semiconductor materials but also emphasizes the role of computational methods in guiding experimental efforts. By systematically exploring the impact of varying selenium concentrations, this study sets a precedent for utilizing computational approaches to inform the design of new materials with tailored properties. Moreover, the findings will contribute to the development of predictive models that can streamline the discovery of novel semiconductors and optimize existing materials for specific applications. As computational tools continue to evolve, this research underscores their importance in bridging the gap between theoretical predictions and practical implementations in materials science, ultimately accelerating innovations in technology.

CHAPTER TWO

LITERATURE REVIEW

Density Functional Theory

A popular computer method for examining the electrical structure and characteristics of several materials, including semiconductors, is density functional theory, or DFT. DFT offers an effective framework for precisely and computationally efficiently examining the basic properties of semiconductor materials.

The electrical and optical characteristics of pristine CdS and Se doped CdS using Density functional theory (DFT) is investigated. A quantum-mechanical (QM) technique for determining the electronic structure of atoms, molecules, and solids is density functional theory. [61] An alternate method to the "HartreeFock plus corrections" paradigm is offered by DFT. It concentrates on the charge density as the fundamental quantity, in contrast to Hartree-Fock or more advanced techniques (Many-Body Perturbation Theory), which are based on the wave function.

The capacity of DFT to precisely forecast the bandgap and electrical structure of semiconductor materials is one of its main features. The effectiveness of DFT in determining the bandgap of popular semiconductor compounds, including silicon (Si), gallium arsenide (GaAs), and cadmium sulfide (CdS), has been shown in a number of investigations [18]. Since the estimated bandgap values from DFT have been demonstrated to closely match experimental data, DFT is a useful method for the design and optimization of materials.

DFT has proven crucial in comprehending the impact of defects and doping on the electrical and optical characteristics of semiconductors, in addition to providing precise bandgap predictions. For instance, the effects of dopants and impurities, such as phosphorus, and boron, on the electronic structure and charge transport properties of Si and CdS have been studied using DFT simulations [19]. These investigations have shed important light on the processes via which doping may alter the characteristics of semiconductors and enhance device functionality.

Band alignment, charge transfer, and other interfacial processes at the junctions of various semiconductor materials, such as CdS/ CdTe and GaAs/AlGaAs, have been studied using DFT computations [20]. For the design and optimization of semiconductor-based devices, such as solar cells, photodetectors, and transistors, these insights into the interfacial characteristics are crucial.

Moreover, DFT has been used to investigate the mechanical, electrical, and structural characteristics of semiconductor nanostructures, including thin films, nanowires, and quantum dots [21]. The understanding of size-dependent effects and the impact of spatial confinement on semiconductor behavior provided by these studies is essential for the development of cutting-edge nanoscale devices.

The dependability and predictive capacity of DFT in semiconductor research have been further strengthened by the ongoing development of DFT methods, including the creation of more precise exchange-correlation functionals and the introduction of many-body phenomena [22]. Consequently, DFT has developed into a vital tool for device engineers and materials scientists, allowing them to more precisely and efficiently design and optimize semiconductor-based technologies.

1. Cadmium Sulfide

With a direct band gap of about 2.42 eV for bulk material, CdS is one of the most significant II–VI semiconductors; both its bulk and thin films can absorb visible light [23]. CdS has demonstrated significant potential in the development of solar cells [24], photodetectors [25], and photo-catalysts [26] due to its exceptional electrical and optical properties, including electron affinity, high absorption coefficient, and low resistivity. To fabricate CdS thin films, a variety of techniques have been employed, including chemical vapor deposition (CVD), chemical bath deposition (CBD) [27], radio frequency (RF) magnetron sputtering [28] and vacuum evaporation method [29], CBD is an inexpensive method that doesn't require a hoover.

CdS is a semiconductor material that has been studied extensively for the use of solar energy [30]. It has a band gap of about 2.4 eV, is inexpensive, has a variety of polymorphs, and excellent optical and electronic properties [31]. According to [32], the intrinsic properties of CdS make it appropriate for a variety of photocatalytic and electro-catalytic processes, including water splitting, CO_2 reduction, organic pollutant degradation, and photocatalytic degradation. For a variety of applications, CdS-base hybrids with distinct materials have shown some great results [33].

2. Selenium

Group VI element Se, is an important semiconductor that offers extraordinary properties, including high photoconductivity, anisotropic thermal conductivity, high piezoelectric and thermoelectric response, etc., which are mainly dependent on its electrical structure with six outer electrons in the

5s25p4 configuration. [34] Se has three stable allotropic forms, an amorphous composed by rings of Se8 (red), a polymeric containing selenium (t-selenium). Se and Te have an electrical arrangement that has been thoroughly examined by Yu and Ye.

3. Doping

In order to improve the electrical, optical, and structural characteristics of CdS and hence the performance of CdS-based devices, doping of CdS has been thoroughly studied.

In order to alter the electrical, optical, and electronic characteristics of semiconductor material, a crucial step in the production of electronic and optoelectronic devices is known as semiconductor doping. This involves purposefully adding impurities to the semiconductor material. A variety of semiconductor-based devices may be developed by carefully controlling the concentration and kind of charge carriers (electrons and holes) in the semiconductor lattice by selectively adding foreign atoms, called dopants.

Doping raises the semiconductor's total electrical conductivity by adding more charge carriers—either electrons or holes—to the material. Semiconductors that are n-type (electron-rich) or p-type (hole-rich) can be produced, depending on the kind of dopant [35]. Development of p-n junctions, transistors, and other electronic components is made possible by the exact control of the doping concentration, which enables tuning of the semiconductor's conductivity [36].

Changes in the bandgap energy of a semiconductor can result from dopant inclusion, which can modify the semiconductor's electrical structure [37]. Optimization of the semiconductor's optical and photocatalytic characteristics, including light absorption, emission, and photocatalytic activity, is possible by bandgap engineering via doping [38]. The bandgap may be shifted by doping to desired energy levels, opening up a larger portion of the electromagnetic spectrum for utilization [39].

Dopants have the ability to introduce many kinds of defects into the semiconductor lattice, including vacancy, interstitial, and substitutional defects [40]. Device performance is highly dependent on the optical, electrical, and recombination properties of the semiconductor, all of which may be strategically controlled [41]. The separation and transit of photo-generated charge carriers may be improved by defect engineering through doping, which raises the general efficiency of semiconductor-based devices and applications [42]. The creation of a vast range of electronic, optoelectronic, and energy-related devices that have revolutionized modern civilization

has been made possible by the exact control and knowledge of doping processes, which have been essential for the growth of semiconductor technology.

4. Doped Cadmium Sulfide

Doped Cadmium Sulfide has been the center of study. Researchers have been studying the optical and electrical properties of pristine and doped Cadmium Sulfide. A density functional study has been done by group of researchers on Cadmium Sulfide doped with various concentrations of Sodium. According to their findings, S atoms (p-orbitals) play a dominating role in TDOS and PDOS, whereas dopant (Na) p-states and Cd d-states contribute. Optical absorption exhibits blueshift when Na content rises, which is consistent with studies from the literature. The dielectric constant rises with concentrations of 3.12% and 6.27% Na but falls at concentrations of 9.37% Na. Therefore, unexpected and surprising findings on the optical characteristics of the CdS: Na system show that this material has the potential to be applied in the fields of dielectric electronics, functional microelectronics, piezoelectric transducers, and nonlinear optics. [43] A different team of researchers looked at the effects of doping zinc with cadmium sulfide. They discovered that because of bonding effects, optical characteristics show different graphical behavior for the two supercell designs (1x1x2 and 2x2x2). The orbitals that contribute most to the conduction process are Cu-4d, S-3p, and Zn-3d. Zn doping in the CdS lattice results in notable changes to its optical and electrical characteristics, enabling a wide range of applications in optoelectronics, optical sensors, and related devices. [3] Another group also used density functional theory (DFT) to study TDOS, PDOS, and optical characteristics of Al doped rocksalt CdS system. The Wien2K code uses the PBE GGA and GGA + U methods to computationally engineer the rocksalt CdS system. Al doping results in strong s–p hybridization and increased conductivity. A number of supercell configurations have been postulated for the replacement of Cd +2 with Al +3 atoms, including 1×1×2, 2×2×1, and 2×2×2 supercell configurations as well as for DFT + U (1×2×2). When comparing the optical absorption of 2×2×1 supercell configuration with DFT + U to 1×1×2 supercell configuration, the former exhibits blueshift, while the latter displays redshift. The optical curves for the 2×2×1 supercell structure differ from the others in that they have a higher refractive index and dielectric constant. The orbitals that contribute are the s-orbitals of Cd, S, and Al. As a result, Al doping improves the opto-electrical characteristics of the rocksalt CdS system. [17]

5. Band gap Engineering

The renowned Shockley transistor patent contains early recommendations for exploiting semiconductor heterojunctions to enhance device performance [44]. A few years later, the idea of a semiconductor with a compositional grade was put up by Kroemer [45]. An energy band gap that changes with position is created by spatially altering the semiconductor's stoichiometry (graded band gap). The electrons and holes are therefore subjected to "quasielectric forces," which are equivalent to the spatial gradient of the valence band edge and the conduction band edge, respectively. One of the first and most basic instances of band-gap engineering is this idea. Band-gap engineering is the process of spatially modifying a semiconductor's band gap or, more broadly, its band structure, in order to produce novel material and device features [46].

Following the first homo-junction semiconductor injection laser demonstrations in the early 1960s, Kroemer proposed that laser action and population inversion could be achieved at much lower current densities through carrier confinement in a low-gap region covered by wide-gap heterojunction barriers [47]. The synthesis of high-quality AlGaAs /GaAs heterojunctions by liquid phase epitaxy enabled the development of a continuous wave (CW) heterojunction laser at 300 K [46]. This opened the path to high-performance lasers for light-wave communications.

The next major development was the development of molecular beam epitaxy (MBE) by Cho and Arthur at Bell Laboratories [48]. Across distances as short as a few tens of angstroms, multilayer heterojunction devices with atomically abrupt interfaces and highly regulated compositional and doping profiles may be created using this epitaxial growth approach. Quantum wells are one type of such structure and a fundamental component of band-gap engineering. These potential energy wells are created by sandwiching two wide-gap semiconductors, such as AlGaAs, between an ultrathin lower gap layer that is either the same thickness or less than the carrier thermal de Broglie wavelength. The depth and thickness of the borehole determine the discrete energy levels' spacing and location [49]. Band discontinuity, also known as the well depth, is the energy difference between the bottom of the conduction bands (or the valence bands in the case of holes) in the two materials. Quantum well lasers and other heterojunction devices are designed with band discontinuities in mind. The field of optical recording can benefit greatly from the use of these lasers. A super-lattice is created if several quantum wells are developed on top of one another and the barriers are made sufficiently thin (usually <50 A) that tunneling between the connected wells becomes significant. Esaki and Tsu first put out this idea at IBM in 1969 [50].

6. Electrical Properties

i. Band Structure

With a hexagonal crystal structure, the more prevalent and stable polymorph of CdS is called greenockite [51]. At ambient temperature, the band gap energy of undoped CdS is generally stated to be between 2.4 and 2.5 eV [52] [51]. A technique that is frequently used to adjust the band gap and other optoelectronic features is doping to create the alloy system [53]. The band gap energy can be lowered by replacing with an element with an outsider element [54].

ii. Density of States

A direct band gap with unique characteristics in the valence and conduction bands characterizes the density of states (DOS) CdS [55]. The number of accessible energy states or levels for electrons in the conduction band and holes in the valance band per unit volume is determined by the density of states, or DOS. P-orbitals often have less intra-band interaction between electrons in 3d orbitals and are hence delocalized in nature [56].

7. Optical Properties

characteristics of optics CdS nanoparticles have revolutionized the field and opened up new avenues for nano-technological development. The optical behavior of CdS is remarkable and attractive because of quantum confinement phenomena. CdS has been a popular window layer material because of this, and it has outstanding uses in the fields of optoelectronics, photonics, and solar energy applications [57] [58] [59] [14].

An experimental investigation on doping CdS with zinc (Zn) revealed that Zn significantly improves its optical characteristics. With an ionic radius of 0.074 nanometer for zinc and 0.097 nm for cadmium, zinc is a valuable element among transition metals. As a result, Zn+2 may readily enter the lattice or crystal of cadmium silver upon replacement [60]. Zn-doped CdS concentrations have been explored by Agbo et al., who also conducted structural studies and concluded that optical characteristics are increased [61]. According to a 2013 study by Foaad et al., blue shifts in the absorption edge occur when zinc levels rise [62]. The study examined the impact of zinc on structural and optical features. Anbarasi et al. reported on an experimental investigation of Zn-doped CdS in [63], including its structural, morphological, optical, and electrical characteristics with the use of spray method. Their results confirm CdS: Zn's candidature as a window material in solar energy cells and suggest it as the best choice for optoelectronic devices. According to

Lakshmy et al.'s [64] research, concentrations and pH levels affect the changes in optical characteristics linked to transmittance and absorption in CdS thin films deposited by chemical bath deposition. In their study, Zn doped CdS nanostructures generated by hydrothermal synthesis were examined by F. Yang et al. They published data from XRD, SEM, XPS, and absorption, noting that Zn concentrations in CdS significantly alter optical characteristics [65]. Additionally, their practical results, taking into account the wurtzite structure of CdS as described in the same paper, agree with the theoretical DFT analysis by VASP. Their research highlights CdS's strong oxidative capacity and demonstrates improved photocatalytic activity that is stable in the presence of visible light.

The previous researches done by various researchers were mainly on doping with different elements other than Se. Doping CdS with Na, Zn and Al have positive impact on the electrical and optical properties of Cadmium Sulfide. Based on the experience of the previous researches I decided to change the dopant and studied the effect that the dopant has on the electrical and optical properties associated with introducing an outsider with pristine cadmium sulfide.

Compound	Dopant	Optical Properties
CdS	Na	Reflectivity, Refractive index, Dielectric constant are improved between the range of 0eV to 2eV.
CdS	Zn	Absorption, Reflectivity, Conductivity, Refractive index, Dielectric constant are improved between the range of 4eV to 6eV.
CdS	Al	Absorption, Reflectivity, Conductivity, Refractive index, Dielectric constant are improved between the range of 0eV to 5eV.

Table 1: List of previous researches done

CHAPTER THREE

COMPUTATIONAL METHODOLOGY

3.1 Material Selection

The host material is CdS, which has a significant optical absorption and an adjustable bandgap. Selenium (Se) can dope it to improve its characteristics. Investigating different Selenium doping concentrations in CdS enables evaluation of their effects on electrical and optical properties. We used space group P 63 m c to mimic a supercell symmetrically. For this research 1.85%, 6.25%, 12.5% and 25% of Se concentration is doped. [42] Selenium is selected as a dopant as a result of its similar properties with sulfur and the two has similar atomic radii. [66] In order to promote successful doping, structural analysis is required to examine the crystalline structure and lattice compatibility between S and Se. Beside with optical properties, it's critical to pay attention to vital electrical characteristics like band structure. Ultimately, a thorough grasp of the characteristics of selenium-doped CdS will be achieved by using DFT software, Quantum ESPRESSO.

3.2 Computational Setup

DFT Framework

DFT is a quantum mechanical modelling technique used to examine a material's electrical structure. Selenium (Se) is added as a dopant to change the properties of CdS, which serves as the host material due to its broad bandgap and valuable optical properties. For the computations, software database ESPRESSO is used. For general applications, a suitable exchange-correlation functional, PBE, is crucial. The crystal structure of CdS is downloaded from Crystallographic open database (COD), and by substituting the S atoms with Se, a supercell is formed. A dense k-point mesh and an appropriate plane-wave energy cutoff, are important computational parameters. The electronic characteristics, such as band structure and density of states, are computed after the optimization of the doped structure's shape. Lastly, optical properties are determined.

Software Selection

Quantum Espresso

A complete software suite for first-principles simulations, Quantum ESPRESSO is especially made for electronic structure, simulation, and optimization research. It provides precise and effective material property modelling by utilizing pseudopotentials (PP), a plane wave (PW) basis set, and density functional theory (DFT). The IOM-DEMOCRITOS project, which was carried out

in cooperation with a number of prestigious institutions, including the International Centre for Theoretical Physics (ICTP), CINECA Bologna, École Polytechnique Fédérale de Lausanne (EPFL), Princeton University, Paris VI, and IJS Ljubljana, is responsible for the creation of Quantum ESPRESSO. Because of this cooperative effort, Quantum ESPRESSO has become a major instrument in the area, allowing researchers to precisely investigate complicated materials and processes.

Quantum ESPRESSO's primary objectives are to improve efficiency in relation to modern computer systems and to make progresses in techniques and algorithms. Quantum ESPRESSO strive for to give researchers strong tools for modelling and comprehending the characteristics of materials at the atomic level by concentrating on the development of cutting-edge computational approaches. Furthermore, the framework is made to exploit performance on modern computer designs, securing that users may take advantage of high-speed computing resources to their fullest. With its combined focus on cutting-edge techniques and computational effectiveness, Quantum ESPRESSO is sat as a chief platform in the fields of condensed matter physics and materials research.

Beyond simple Density Functional Theory (DFT), Quantum ESPRESSO has innovative capabilities that include hybrid functional, DFT+U techniques, and nonlocal methods to improve the accuracy of electronic structure calculations. Through the application of Wannier functions, the platform makes it easier to study transport phenomena and allows for a thorough examination of ballistic transport features. Quantum ESPRESSO also enables free energy sampling, which sheds light on phase transitions and thermodynamic stability in materials. Its powerful computational capabilities increase its practicality even further by simulating different spectroscopic approaches to look at material characteristics at a fundamental level. When combined, these cutting-edge qualities make Quantum ESPRESSO a flexible and operative tool for researchers studying intricate material interactions and behaviors.

Key Parameters

Selecting an exchange-correlation functional is crucial; popular functional is PBE (Perdew-Burke-Ernzerhof) for general computations. To add selenium as a dopant, a supercell must be made, usually by replacing a portion of the S atoms. The crystal structure of CdS should be retrieved from trustworthy databases (COD). To guarantee adequate sampling of the Brillouin zone,

computational setup necessitates a dense k-point mesh. Convergence in total energy estimates requires a suitable plane-wave energy cutoff. To evaluate its impact on the material's characteristics, the selenium doping concentration should be adjusted. To give a thorough understanding of the behavior of the doped material, post-optimization calculations of the electronic structure including band structure and density of states as well as optical characteristics are carried out.

3.3 Simulation Procedures

i. Preparation of the Initial Structure

The Crystallographic Open Database (COD), a trustworthy source of crystallographic data, is where the CIF file for CdS is originated. Atomic locations and symmetries, among other crucial information about the crystal structure, are included in this file. The CIF is transformed into a format that is compatible with Quantum ESPRESSO, a popular program for electronic-structure calculations and materials modelling, so that this data may be operated in computational simulations. This conversion procedure guarantees that Quantum ESPRESSO interprets the crystal cell accurately, enabling researchers to run precise simulations and learn more about the material's characteristics, including structural stability and electrical behavior.

ii. Setting Up DFT Calculations

Choosing the right exchange-correlation functional is vital to getting trustworthy results while studying the electrical characteristics of materials. The Perdew-Burke-Ernzerhof (PBE functional is used for this purpose because it effectively represents the key features of electrical interactions in a variety of systems. PBE is a popular option for researchers due to its renowned balance between accuracy and computing efficiency. By using this functional, the calculations can precisely account for the effects of electron exchange and correlation, increasing the precision of the outcomes.

iii. Defining Computational Parameters

Setting a thick k-point mesh is crucial for precise Brillouin zone sampling and finding reliable results in electronic structure simulations. More thorough study of the electronic states is made probable by a clearly defined k-point grid, which improves the correctness of energy estimates and

other material features. The combination across the Brillouin zone is enhanced and numerical faults are reduced by increasing the density of the k-point mesh. In the end, this approach adds to more solid and substantial conclusions in computational research by improving the convergence of the calculations and proposing a clearer image of the material's electrical behavior.

iv. Geometry Optimization

A vital stage in computational materials science is geometry optimization, which targets to moderate forces acting on atoms and relax the structure. In order to confirm that the system enters a stable state, atom locations are changed iteratively until a configuration that matches to the lowest potential energy is established. Because it avoids any false stress or instability in the structure that can distort further examinations, this optimization phase is vital. Researchers may assuredly move on to other studies, such electrical structure calculations or property calculations, by forming a well-relaxed configuration, which will produce more accurate and dependable conclusions.

v. Electronic Structure Calculations

The band structure and density of states (DOS) must be determined in order to examine the doped material's electrical characteristics. The band structure tells facts about the valence and conduction bands and the energy levels that electrons may access. In the meanwhile, the DOS demonstrates the distribution of electronic states at diverse energy levels, presenting the number of states that electrons can inhabit. Researchers can realize how doping affects the material's electrical behavior, including differences in conductivity and energy gaps, by combining these computations.

vi. Optical Properties Calculation:

Accurate findings in material science required the use of density functional theory (DFT) simulations to derive optical parameters such as optical absorption, reflectivity, loss function, optical conductivity, dielectric function, and refractive index. Predicting how materials would react to electromagnetic radiation required the precise computation of electronic structures, which DFT's quantum mechanical framework made possible. Researchers successfully modelled the interactions between light and matter by using DFT simulations, which provided insights into the optical behavior of materials. In addition to improving our knowledge of basic optical processes, this method helped create cutting-edge materials for a range of uses.

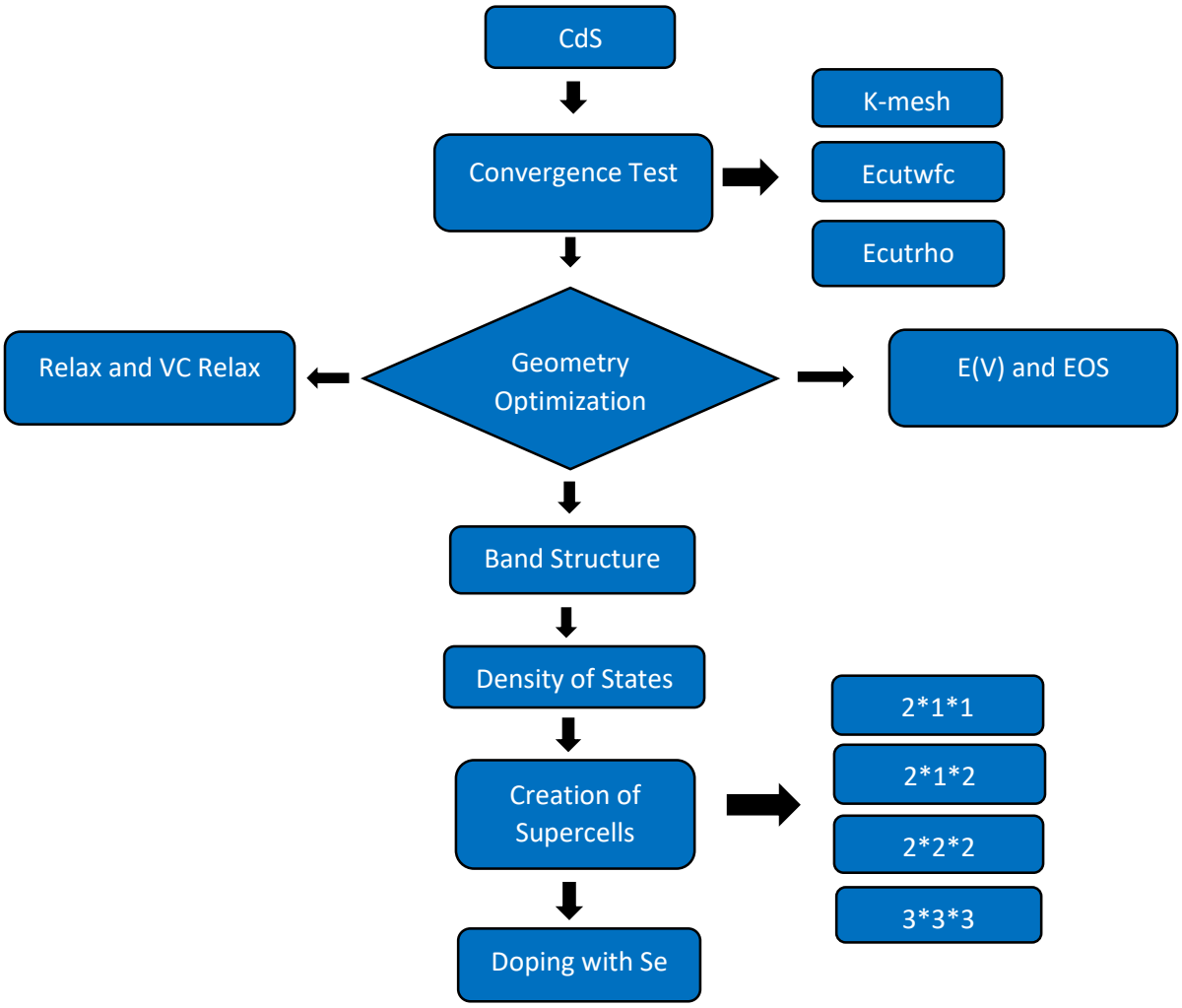
CdS
Convergence Test
K-mesh
Ecutwfc
Ecutrho
Geometry Optimization
Relax and VC Relax
E(V) and EOS
Band Structure
Density of States
Creation of Supercells
2*1*1
2*1*2
2*2*2
3*3*3
Doping with Se

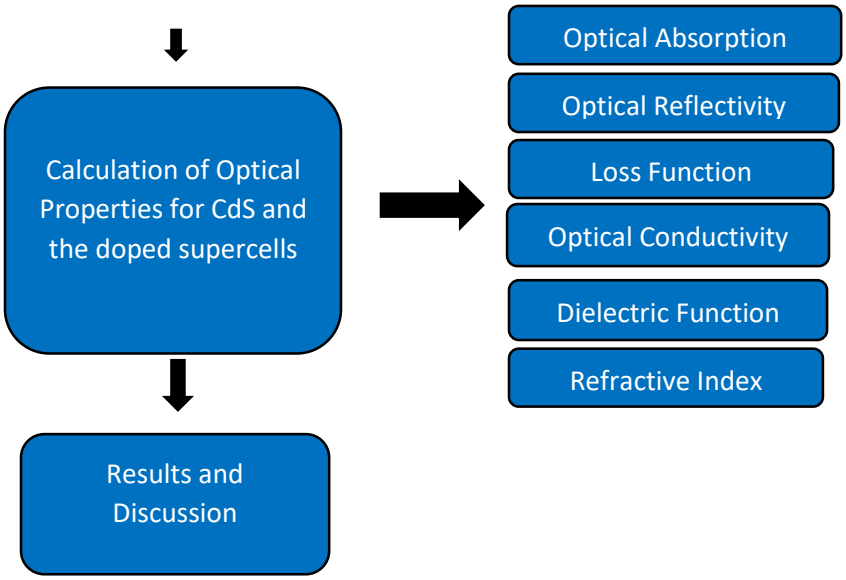

Figure 1: Procedures to analyze electronic and optical properties of CdS and CdS doped Se using DFT simulations.

3.4 Validation Approach

By contrasting the density functional theory (DFT) computations of characteristics with the available actual observations, the findings were confirmed. In order to evaluate the computational model's correctness and make sure that the theoretical predictions and the observed data agreed, this comparison was essential. Researchers determined the advantages and disadvantages of the DFT technique by examining differences and parallels between the computed and experimental outcomes. The dependability of predictions pertaining to material qualities and behaviors in real-world applications was eventually improved by this validation.

The findings were contrasted with density functional theory (DFT) analyses of dopants and cadmium sulphide (CdS) that had already been published. A better understanding of the differences in computed attributes was made possible by the benchmarking method, which was crucial in pointing out differences between various research. Researchers could confirm the validity of the selected computational techniques and guarantee their dependability by comparing results with previous studies.

CHAPTER FOUR

RESULTS AND DISCUSSION

1. Convergence test

Convergence testing is a method for optimizing simulations to make effective computer resources and yield reliable results. To find the essential parameters to get the best energy, I run a number of SCF calculations in this study for the k-points grid, kinetic energy cutoff, charge density cutoff, and lattice parameter optimization. [67]

i. K- point optimization

In the past, computational research concentrated on finding computationally affordable set of k-points for Brillouin zone sampling so that calculations for large-atom real-space unit cells could be completed. However, a more accurate collection of special k-points ought to be utilized for accurate calculations. To get more accurate findings, more grid points can be obtained, however the computation cost increases with this. [68]

SCF computations on the total energy were performed for a range of k-point grids, from 1×1×1 to 15×15×15. As seen in Figure, the total energy fluctuates based on the shift in k-points and eventually converges. The total energy and k mesh values converged linearly starting from 3x3x3.

The ideal set of k-point values chosen for CdS, with a notably modest total energy change, is 7x7x7, taking into consideration the constraints of computer power.

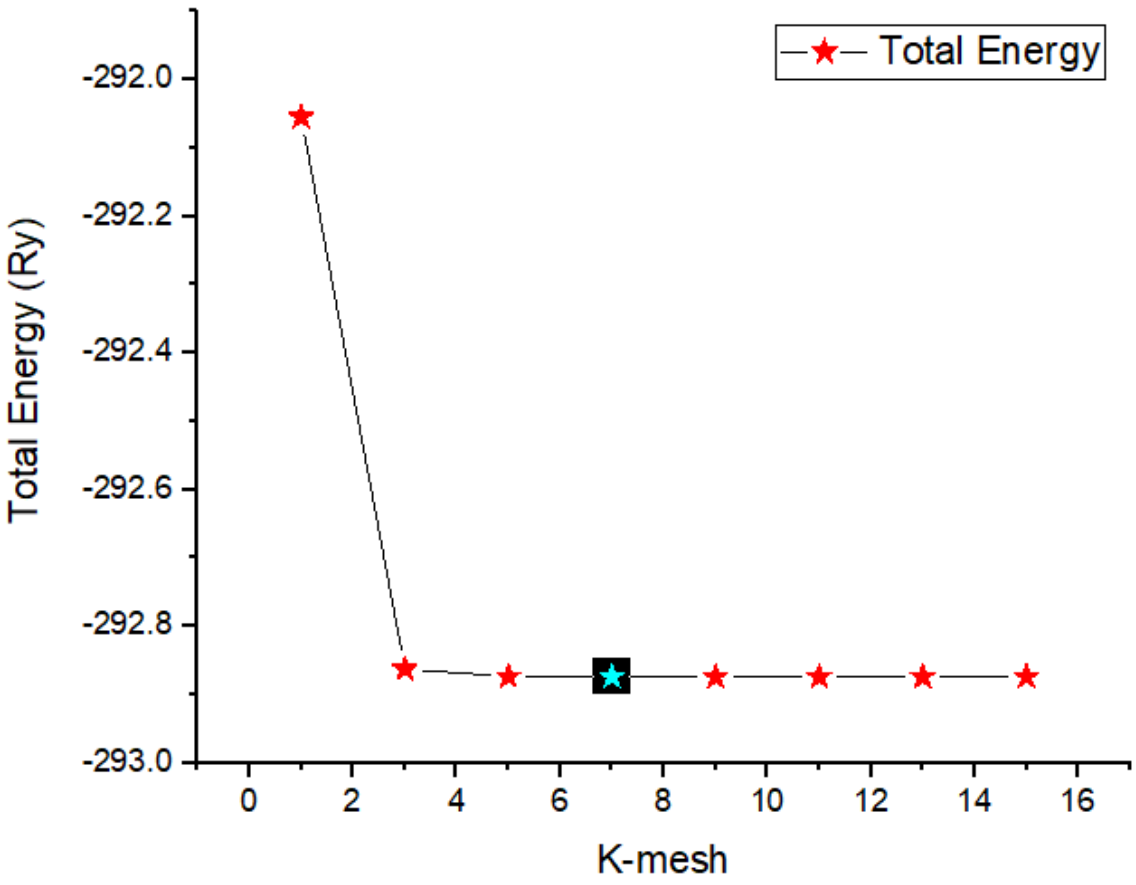

Figure 1: Converged K-points

ii. Basis set size optimization

Ecutwfc indicates the wave function kinetic energy cutoffs, while Ecutrho indicates the charge density cutoffs. The number of plane waves that Ecutwfc specifies can be used to determine the DFT. When the value for the computation of plane waves is set to a big number, the calculation accuracy rises but the calculation time increases. It is necessary to modify the number of plane waves in order to get the proper balance between the maximum kinetic energy cutoff and the number of waves. It is crucial to maintain Ecutrho as one of the several elements of Ecutwfc during computation. Next, we can adjust it initially while keeping Ecutrho at the same factor time as

Ecutwfc. Once the right value for Ecutwfc has been found, the process is also done for Ecutrho. [69]

a. Ecutwfc

In order to improve computational performance in plane-wave computations, the ecutwfc parameter is optimized at 50 Ry. This configuration ensures that the simulations provide accurate results without incurring undue computing expenses by striking a balance between accuracy and resource utilization. Users can attain efficient performance in electrical structure computations by optimizing at this value.

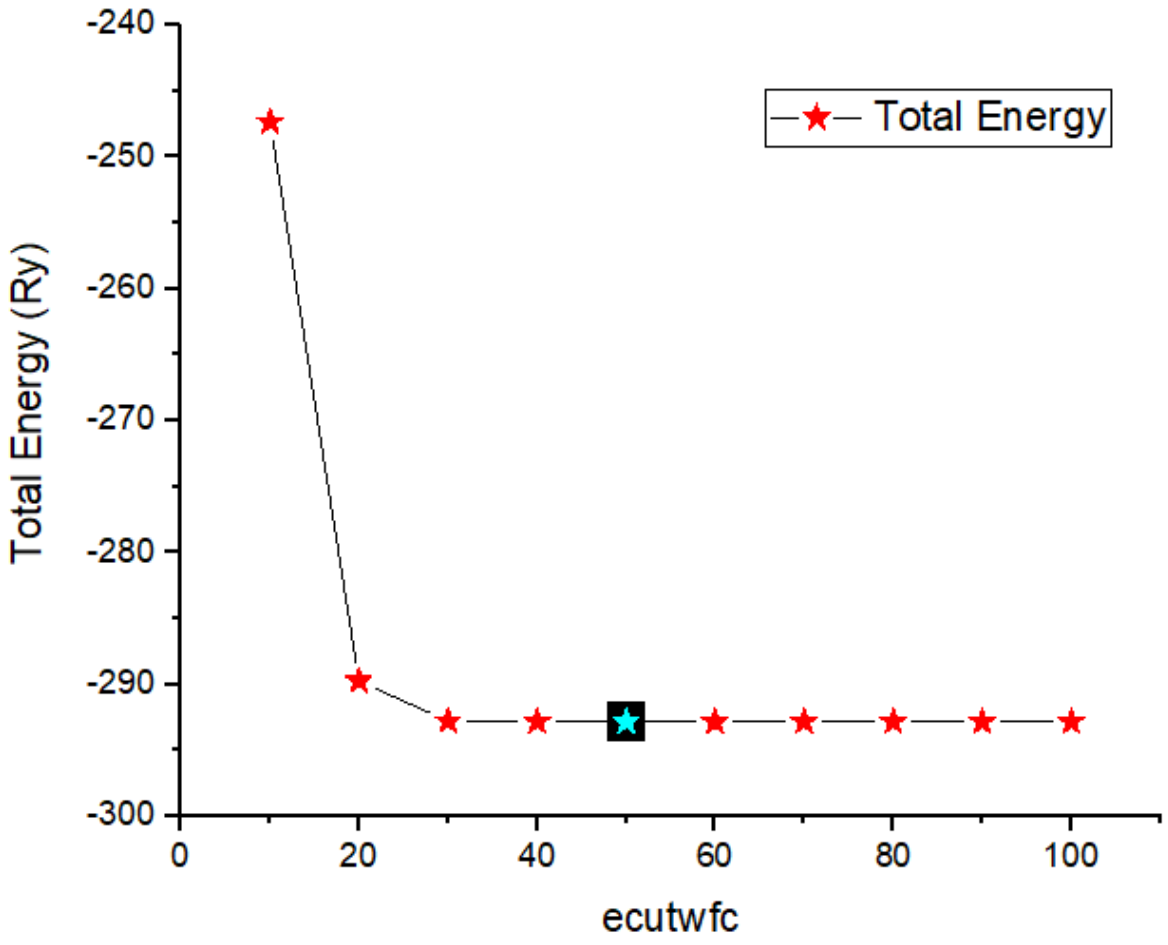

Figure 2:Converged ecutwfc

b. Ecutrho

To increase the accuracy of charge density estimates in electronic structure simulations, the ecutrho parameter is set to 200 Ry. More precise representation of the wave function's finer features is guaranteed by this optimization, producing more trustworthy outcomes. It strikes a compromise between the requirement for high-quality results in material modelling and computing economy.

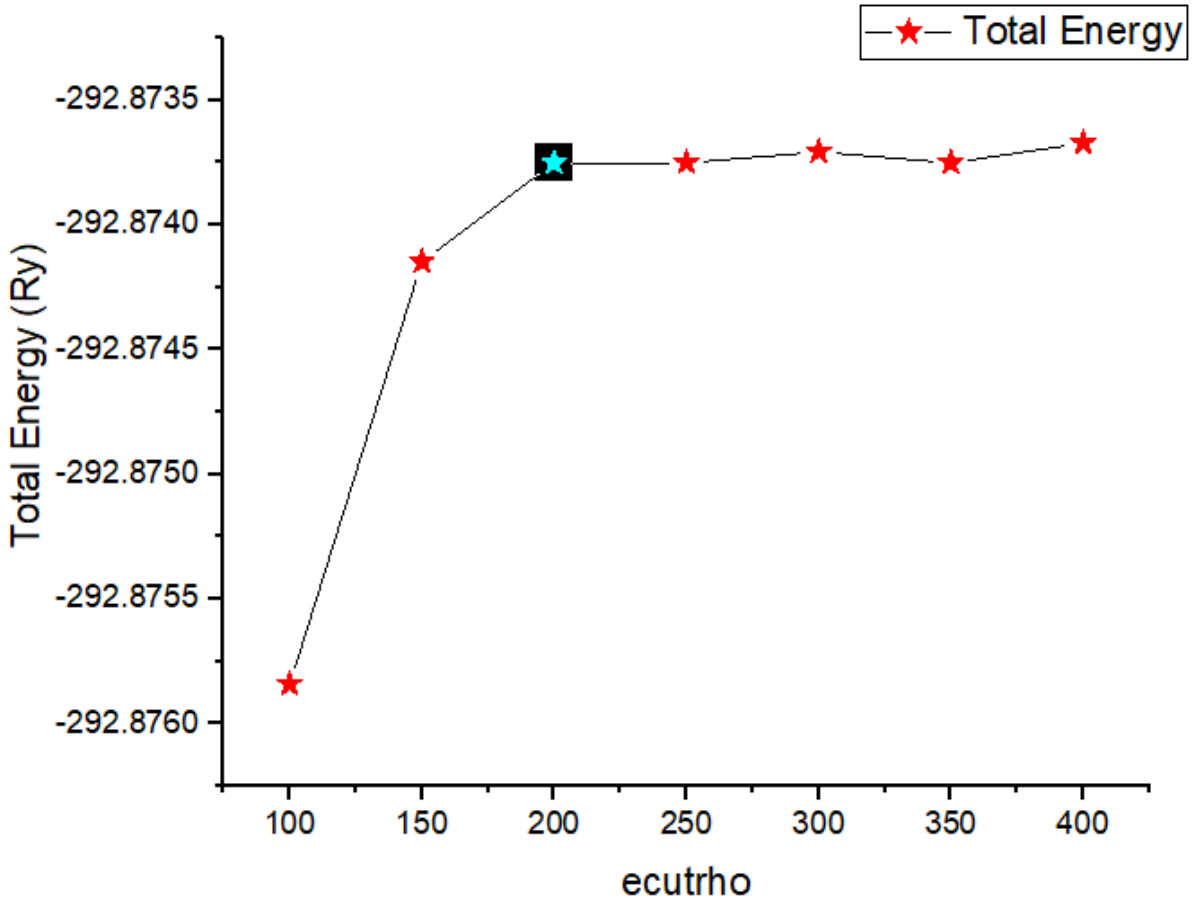

Figure 3: Converged ecutrho

iii. Lattice constant Optimization

CdS lattice constant optimization was performed by giving a starting lattice constant that was smaller than the experimental value while calculating its total energy. I did the computations again, and at the conclusion of each step, I received new total energy and lattice constants. I kept going till I had the lattice parameter with the lowest possible overall energy. To get a stable atomic location for the subsequent computation, the crystal structure must be relaxed after getting the minimal total energy and optimized lattice constant. [68]

The exact minimum value of the total energy is found to be at -292.8760214 Ry. At this specific point the lattice constant point becomes 4.237 Å.

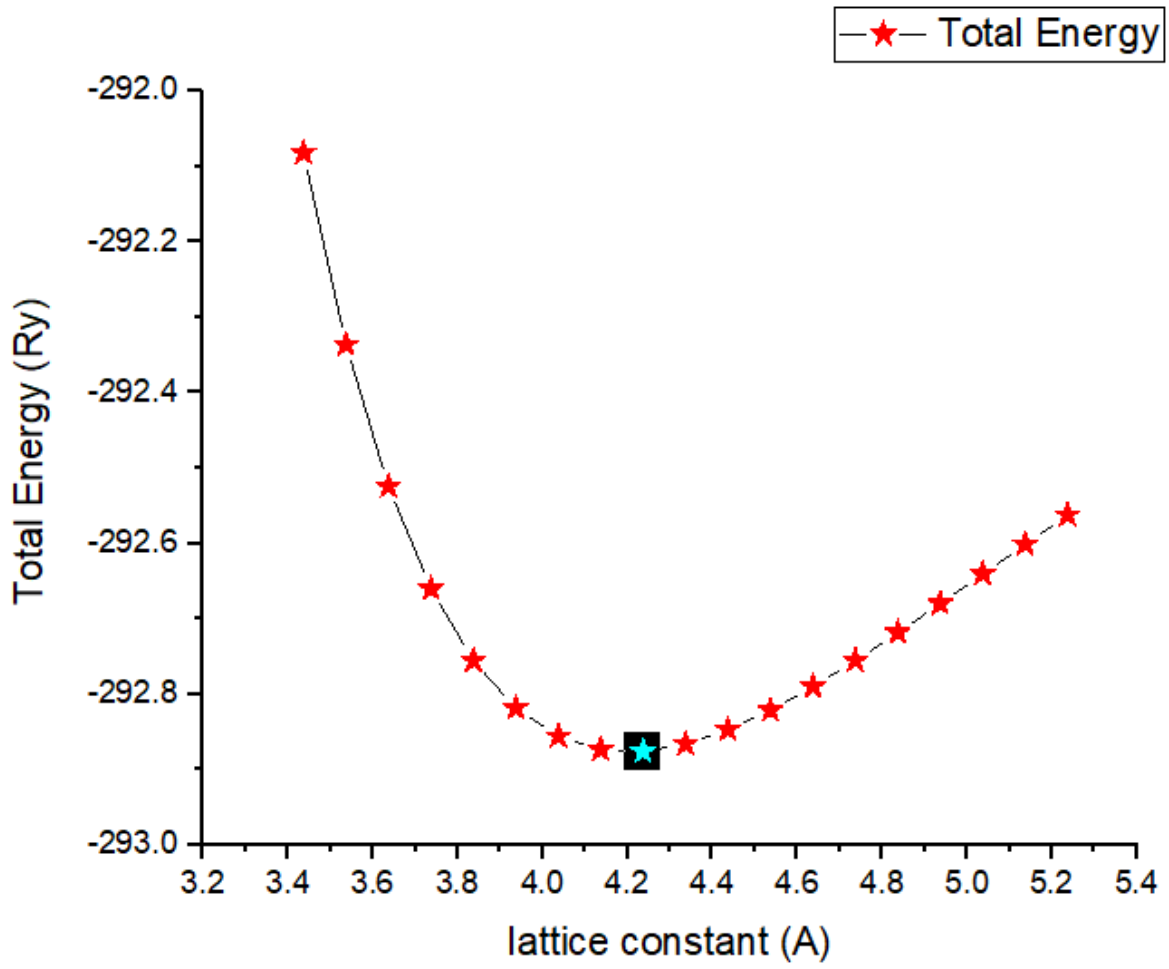

Figure 4: Approximated Lattice Constant

2. Doping with Selenium

I chose these concentrations by using a research done on CdS doped by Na using dft. The researchers used 3.12% to 9.37% concentrations of dopants. They got improved electrical and optical properties for these concentrations.[42] I also chose a closer values starting from 1.85% to 25% dopant concentration. The upper concentration is to check what happens at heavy dopant concentration. I created different supercells [2*1*1] 25% Se dopants, [2*1*2] 12.5% Se dopants, [2*2*2] 6.25% Se dopants and [3*3*3] 1.85% Se dopants. Then I changed one of the four sulfur atoms with selenium as shown in the following figure for [2*1*1] supercell. Followed by changing one of the eight atoms of Sulfur with Selenium for [2*1*2] supercell. After that I changed one of

the sixteen Sulfur atoms with Selenium for the [2*2*2] supercell. Finally, I changed one of the fifty-two Sulfur atoms with Sulfur for the [3*3*3] supercell.

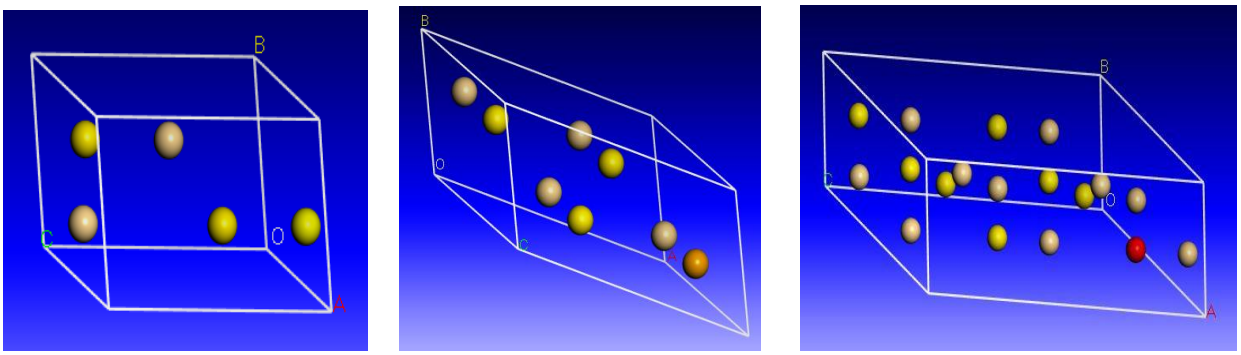

a) Pristine CdS **b)** CdS doped Se [2*1*1] **c)** CdS doped Se [2*1*2]

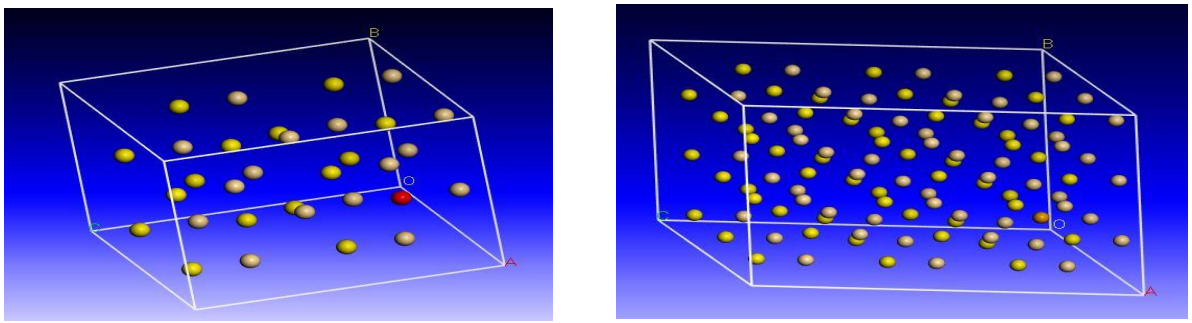

d) CdS doped Se [2*2*2] **e)** CdS doped Se [3*3*3]

Figure 5: 3D representations of Supercells

3. Electronics structure calculations of CdS and CdS doped with Se

i. Band Structure

In accordance with experimental findings, the band gap of CdS reduces linearly with increasing selenium concentration. It is discussed how the concentration of selenium affected the valence and conduction band margins. [61] It's also discovered that variations in the band dispersion and nature of the valence and conduction bands occur in tandem with the lowering of the band gap with an increase in selenium concentration. [20]

The paths used for the diagrams are generated by the supercomputer. Similar paths were attempted for all the diagrams, but it became too expensive in terms of computation, as the calculations took months and still did not finish.

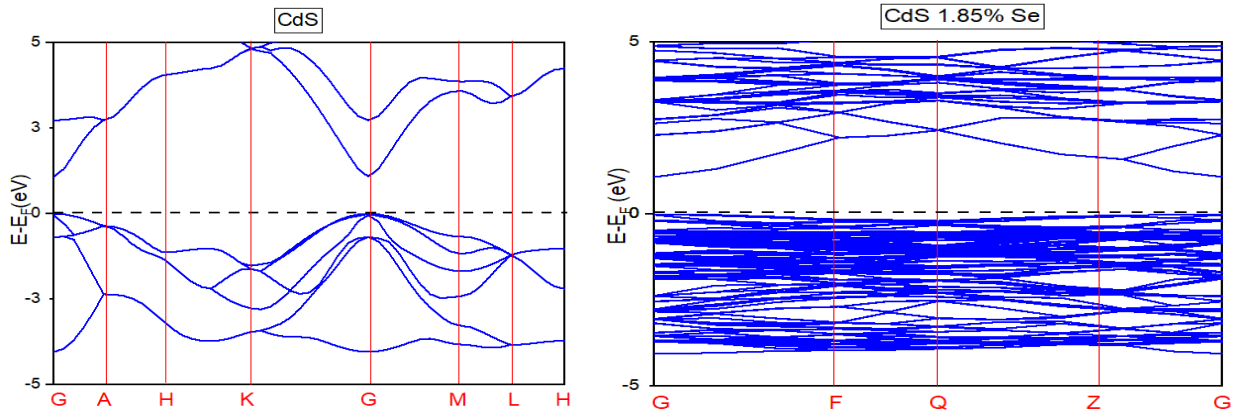

a) Pristine CdS

b) CdS doped Se [3*3*3]

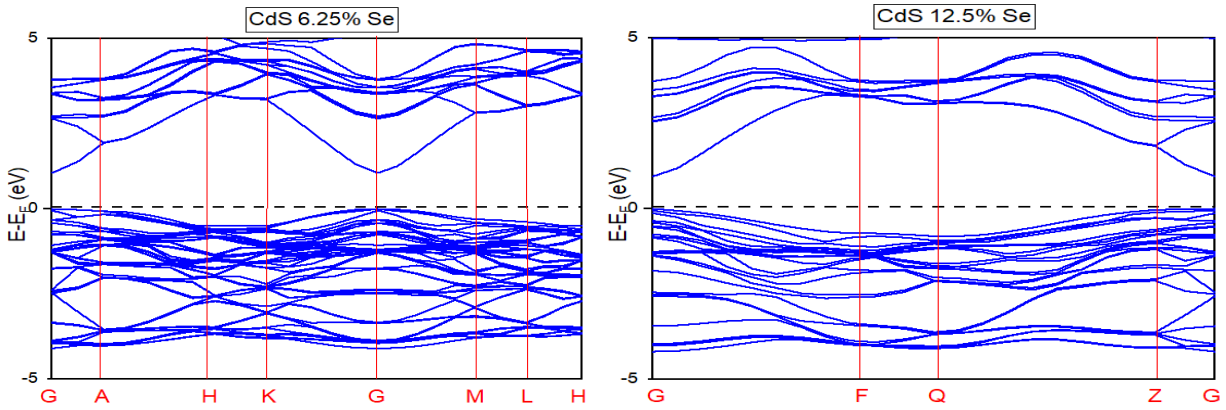

c) CdS doped Se [2*2*2]

d) CdS doped Se [2*1*2]

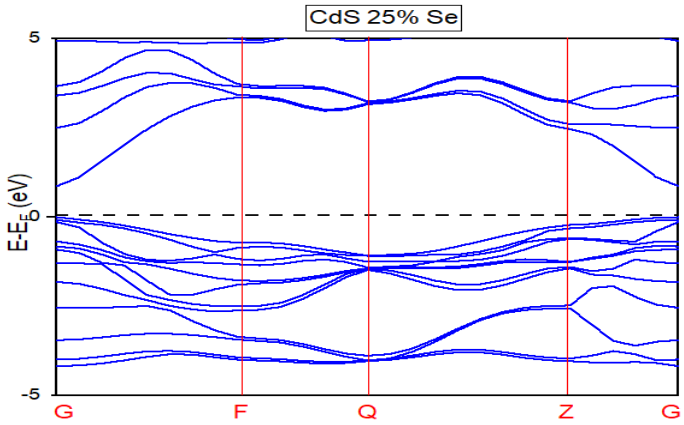

e) CdS doped Se [2*1*1]

Figure 6: Electronic Band Structures of Pristine and doped Supercells

Compound	Calculated Band-gap	Literature
Pristine CdS	1.089 eV	1.15 eV to 1.37 eV (PBE)
CdS 1.85% Se	1.083 eV	
CdS 6.25% Se	1.058 eV	
CdS 12.5% Se	0.952 eV	
CdS 25% Se	0.871 eV	

Table 2: Calculated band gap for Pristine CdS and supercells doped with Se Vs literature [70]

The key findings from these DFT-based studies on the band structure can be summarized as:

- The valence and conduction band edges fluctuate in tandem with changes in the band gap, enabling the electronic characteristics to be tuned.
- The band gap decreased as the doping concentration of Se increased. [71] The decrease in band gap energy with increasing concentration doping is a result of the influence of doping-induced defects and impurity bands on the electronic structure of the materials.

ii. Density of States

The density of states predicts state occupancy over a certain energy interval and offers information about the electron's shift from the valence to the conduction band. DOS is not an unchanging, fixed amount determined by nature. It is altered to enhance device performance [72]. Figure.8 show the total density of states, with the Fermi level shown by a dotted line.

The supercell with the highest number of atoms which is 1.85% Se has higher TDOS which is about 750 arbitrary units. For the second highest supercell with the second highest numbers of atoms which is 6.25% Se, the PDOS is about 220 arbitrary units. Finally, for pristine CdS the numbers of atoms are 8 and the PDOS significantly decreased to around 20 arbitrary units. According to Kohn Sham 1996 density of states scale linearly with the number of atoms. [73]

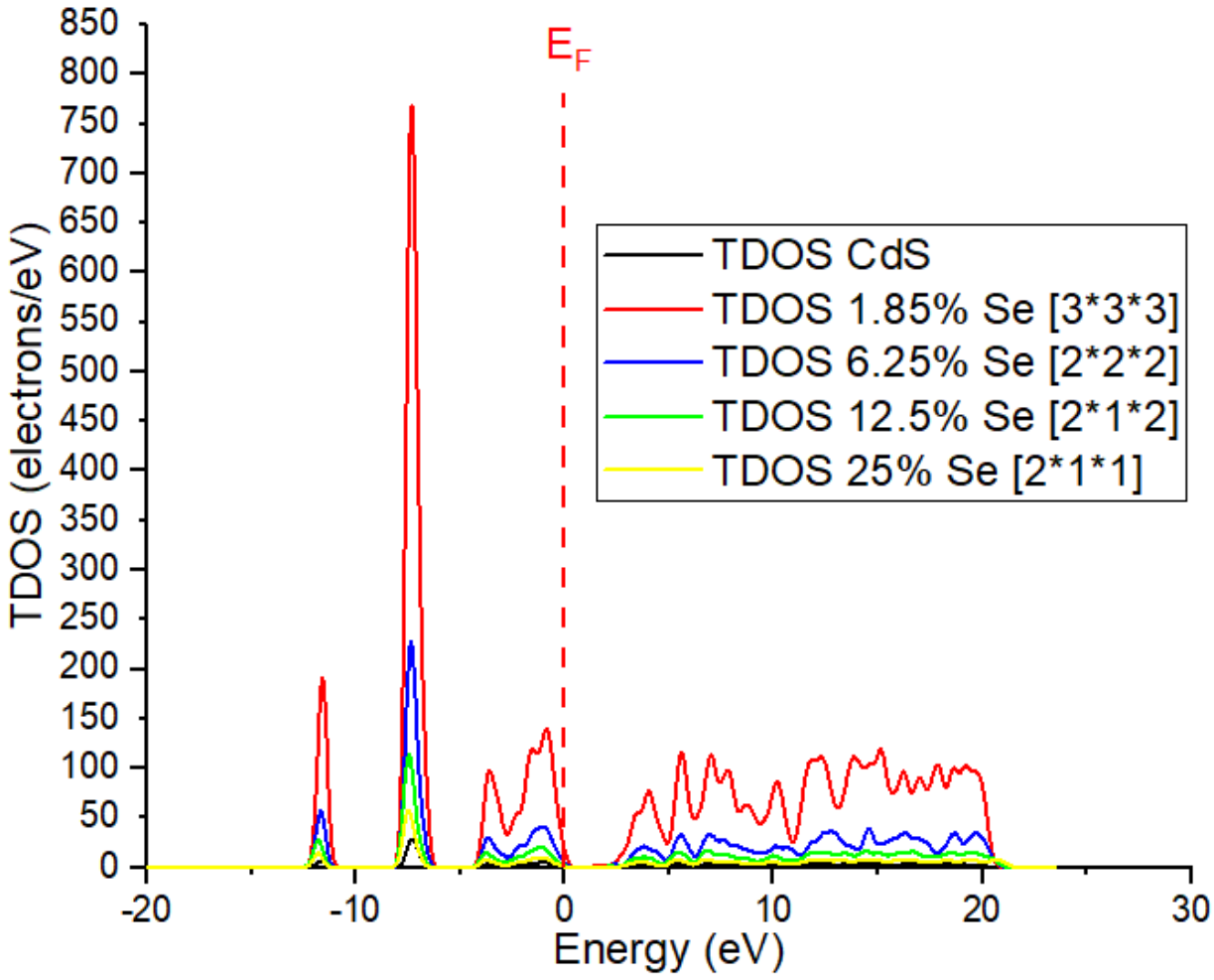

Figure 7: TDOS for pristine CdS and doped Supercells

4. Optical Properties

i. Optical Absorption

Absorption spectra are analyzed in the energy range of 0–35 eV and interpreted in a wide range of electromagnetic spectrums. This spectrum was caused by electron excitations from the valence to the conduction band [74] and quantum confinement effects, which become significant after doping [75] [76]. The quantum confinement effect also contributes to the migration of absorption maxima towards areas of lower wavelength [76]. This may be explained by assuming that transition dipole orientations are random with respect to the direction of the stimulating electromagnetic field [77].

Furthermore, absorption patterns are nearly identical for different Se concentrations, with a modest shift in the absorption edge towards higher energy values and a broadening as dopant concentrations increase. The widening of these peaks might have an explanation related to

impurity inter-band transitions [57] [78]. When compared to pure CdS, the absorption maxima at all concentrations exhibit shift and are moved towards the high energy area. Therefore, when dopant concentrations in the host CdS lattice grow, we get a shift in the absorption spectrum. Shift indicates strong bonding and the interaction of dopant (Se) atoms with CdS [79].

The absorption for the supercells other than the 6.25% Se doping concentrations are somewhat similar. On the other hand, for the 6.25% Se, the absorption peak increased a little over the 25,000 cm^{-1} for the pristine CdS and the other doped supercells the absorption is a little under 25000 cm^{-1}. The other thing is that the remaining peaks shifted a little bit to the right and to the left for the doped supercells.

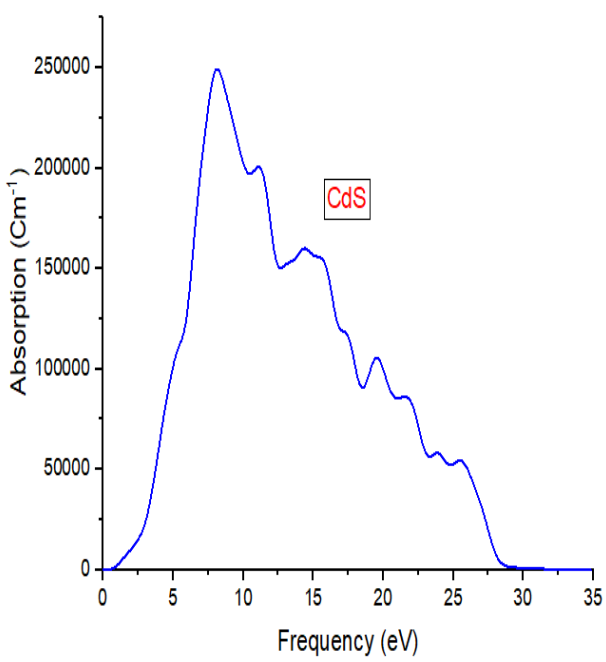

a. CdS

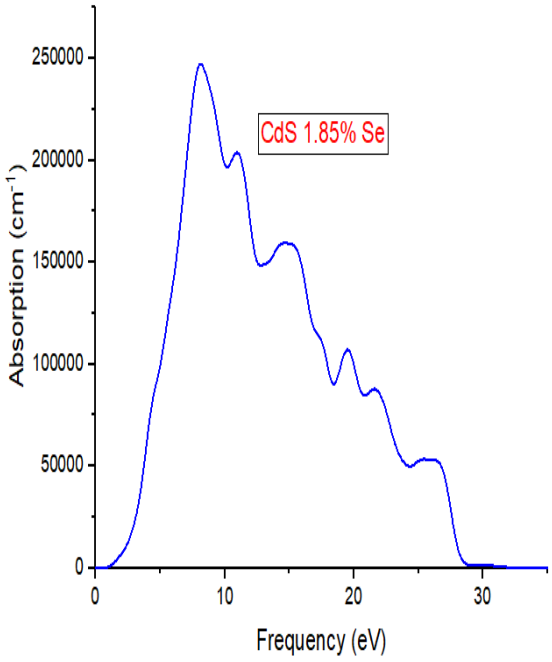

b. CdS 1.85% Se

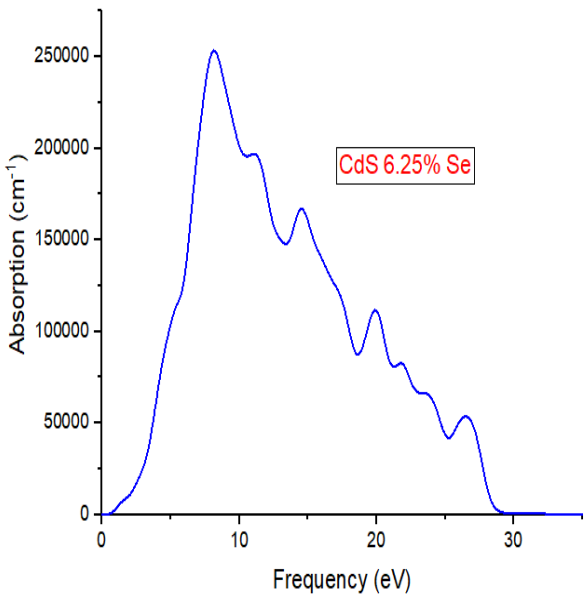

c. CdS 6.25% Se

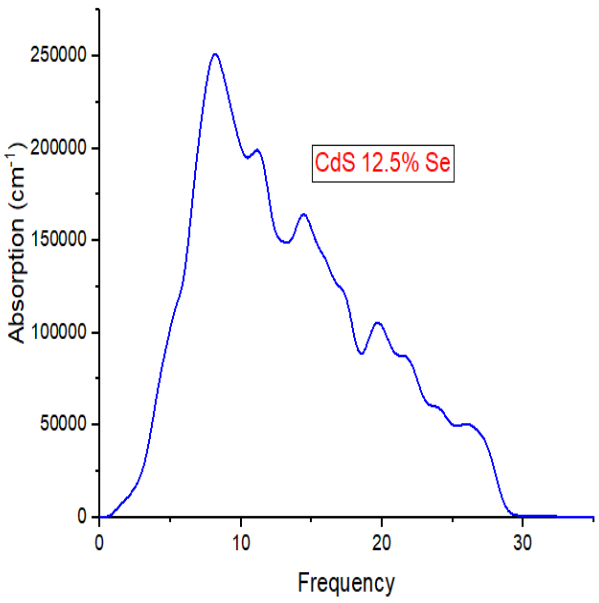

d. CdS 12.5% Se

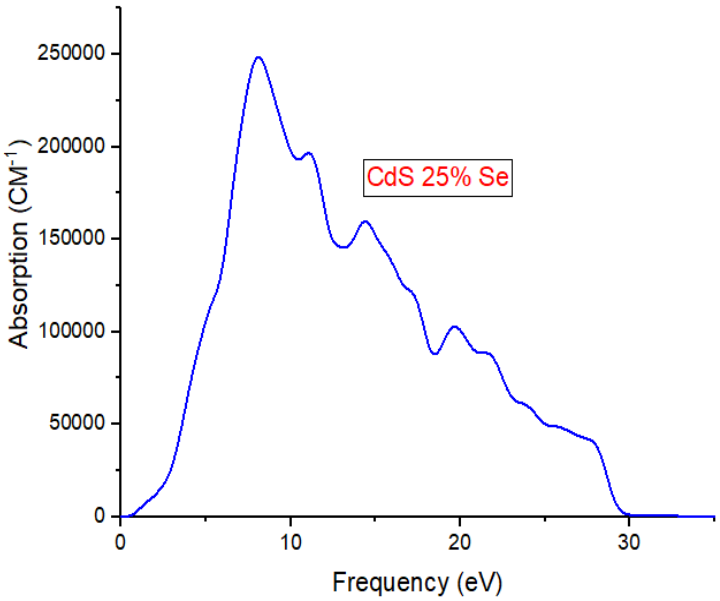

e. CdS 25% Se

Figure 8: Calculated Optical absorption for individual Pristine CdS and doped Supercells

The highest absorption point is for the dopant concentration of 6.25% Se around 8eV in Fig.9 c). The other peaks recorded for this concentration are at 14.5eV, 20eV and 22eV. For dopant concentration of 1.85% (Fig.9 b)) the absorption peak is also observed at 8eV but has lower

absorption than 6.25% of Se. Other peaks observed for 1.85% Se are at 11eV, 15eV, 19eV, 22eV and 26.5eV. For pristine CdS (Fig. 9 a)) the peak absorption is also observed at 8eV. Other notable lower peaks are observed at 11.5eV, 14.5eV, 19.5eV, 23.5eV and 25.5eV. For the 12.5% concentration of Se (Fig.9 d)) the peak point is also observed at around 8eV. Other observed lower peaks points for this concentration are at 11.5eV, 14.5eV, 20eV and 22eV. Finally, for the 25% dopant concentration (Fig.9 e)) the peak point is also observed around 8eV. Other lower notable peak points are at 12eV, 14.5eVand 20eV. The peak for Zn doped CdS optical absorption is enhanced at the range of 4eV to 6eV. The peak for Al doped CdS optical absorption is enhanced at the range of 4eV to 5eV. The peak for Na doped CdS optical absorption is enhanced at the range of 0eV to 2eV.

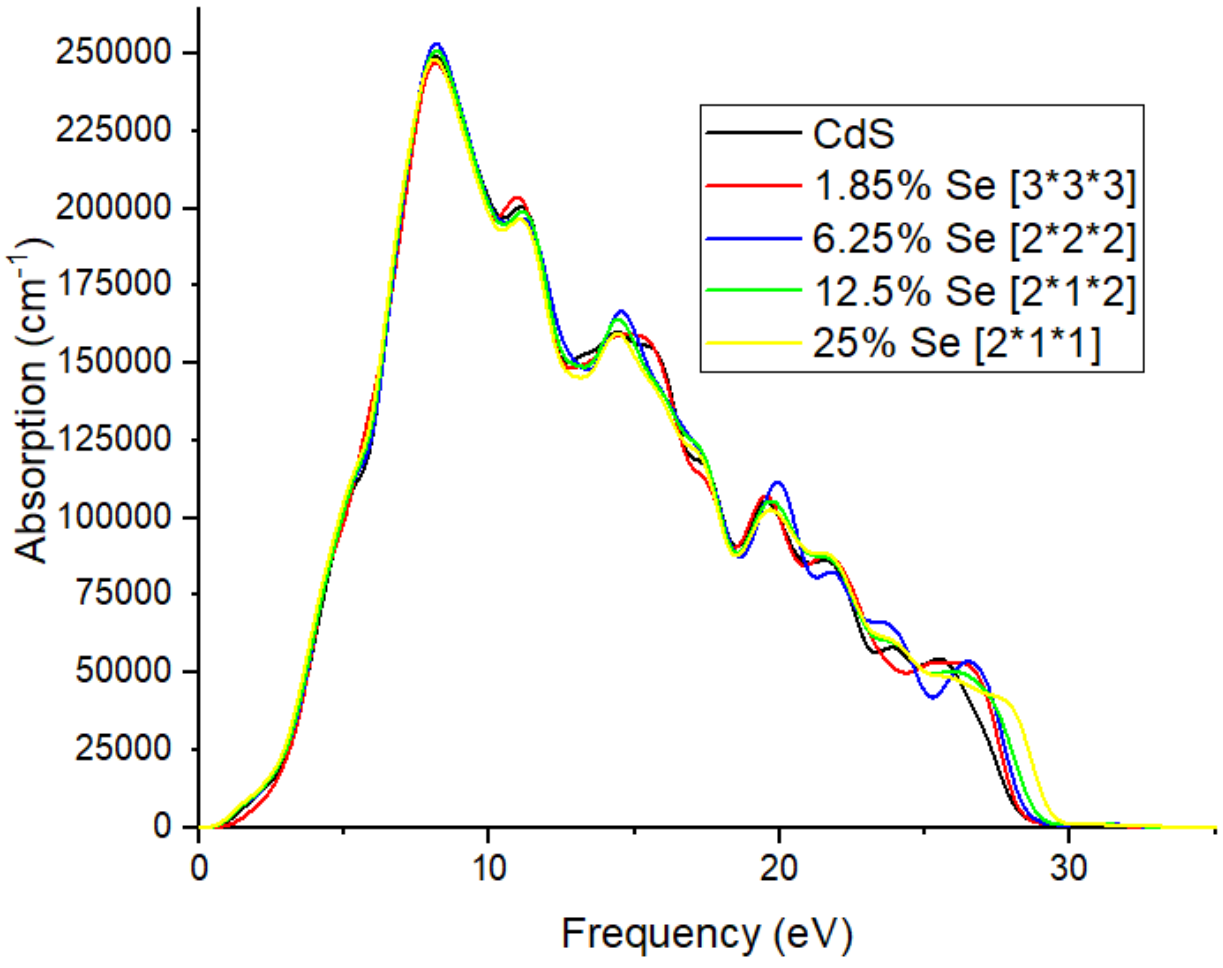

Figure 9: Combined Optical Absorption

ii. Optical Reflectivity

It's discovered that adding selenium increases optical reflectivity, especially for CdS doped Se 6.25%, 12.5% and 25%. Reflectivity increases from 0.42 to 0.44 (arbitrary units).

Inter-band transitions from the valence to the conduction band give rise to reflectivity peaks for all concentrations of Se, which are associated with plasmons. One possible explanation is that oscillations are generated collectively by free electrons [80]. The outstanding reflection behavior of CdS material makes it suitable for usage as a transparent window material.

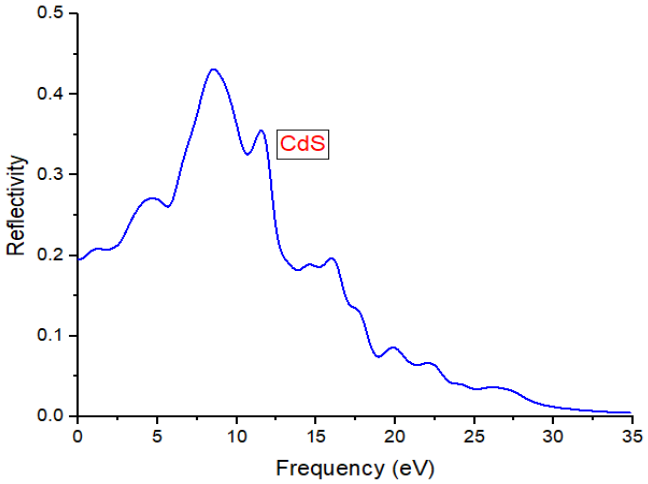

a. CdS

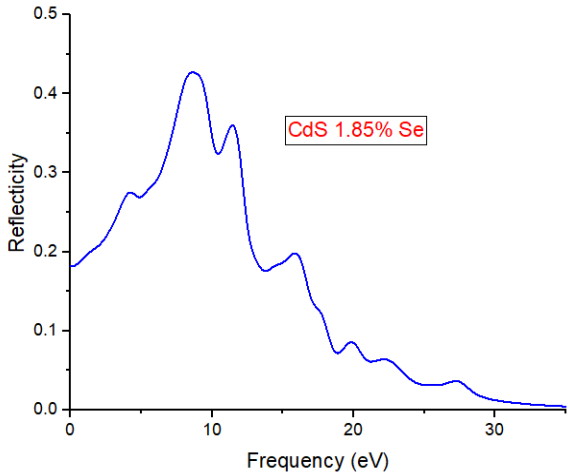

b. CdS 1.85% Se

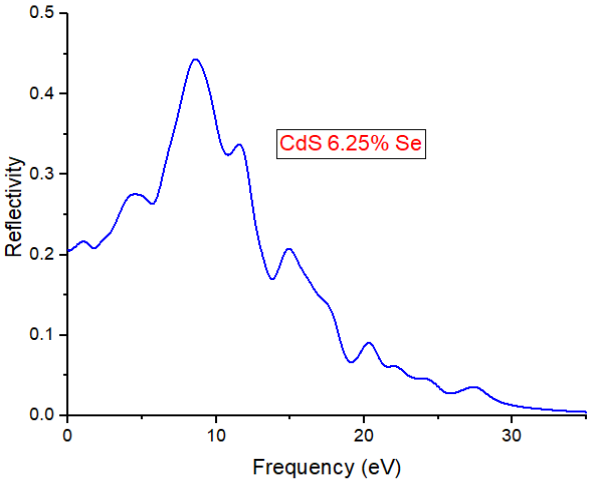

c. CdS 6,25% Se

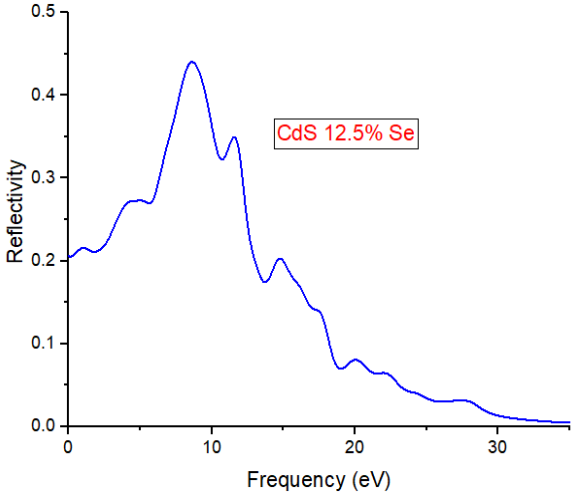

d. CdS 12.5% Se

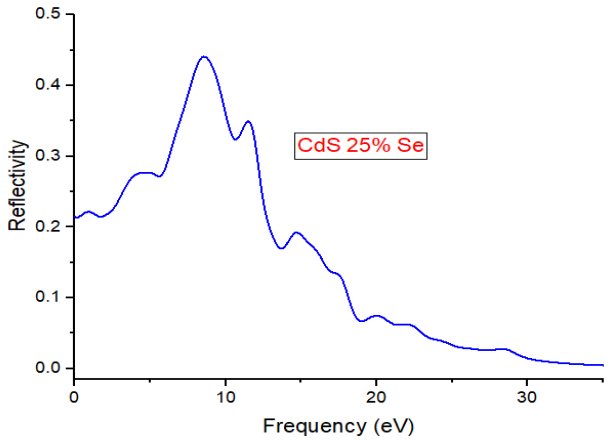

e. CdS 25% Se

Figure 10: Calculated Optical Reflectivity for individual pristine CdS and doped Supercells

At 0eV optical reflectivity of pristine CdS is about 0.19. The highest optical reflectivity at 0eV is observed for 25% Se doped followed by (12.5% and 6.25%) are quite similar, Pristine CdS and 1.85% doped which have 0.22, 0.21, 0.19 and 0.175 respectively. For the pristine CdS (Fig.11 a)) The peak optical reflectivity is observed at 8eV. Other observed lower peaks are at 1eV, 5eV, 11.5eV, 14.5eV, 22eV and 26.5eV. The 1.85% Se doped (Fig.11 b)) showed peak at 8.5eV. Other lower peaks for this concentration are observed at 4.5eV, 11.5eV, 16eV, 20eV and 27.5eV. The peak optical reflectivity is observed at 6.25% Se (Fig.11 c)) at around 8eV. Lower peaks are also observed at 1eV, 4.9eV, 14.5eV, 20.5eV and 28eV. The 12.5% Se (Fig.11 d)) doped concentration showed peak at 8eV. Other lower peaks are observed at 1eV, 4.9eV, 12eV, 14.9eV, 20eV, 22eV and 28eV. For 25% Se doped (Fig.11 e)) the peak is also observed at 8eV. Lower peaks are also observed at 1eV, 4.8eV, 12eV, 14.8eV, 20eV and 28.5eV. The Zn-doped CdS optical reflectivity peak is boosted between 4 and 6 eV. The region of 4.5eV to 5eV is where the peak for Al doped CdS optical reflectivity is boosted. The region of 0eV to 1eV is where the peak for Na doped CdS optical reflectivity is boosted.

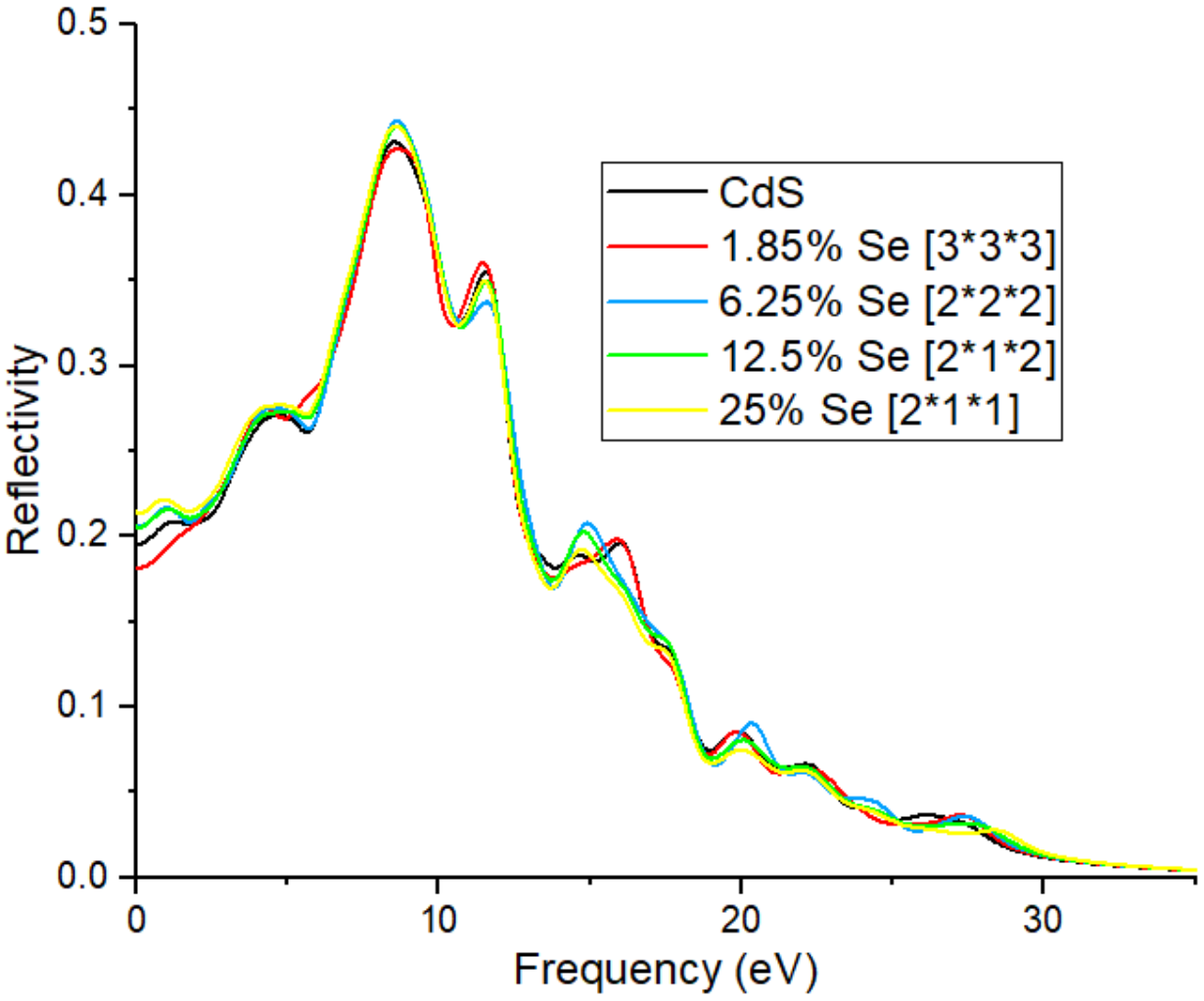

Figure 11: Combined Optical Reflectivity

iii. Loss Function

It's discovered that adding selenium significantly increases Loss Function for all doped supercells, the highest is for CdS doped Se 12.5%. For pristine CdS the peak was at about frequency of around 18 eV but doping shifted the peak to 20 eV for the supercells.

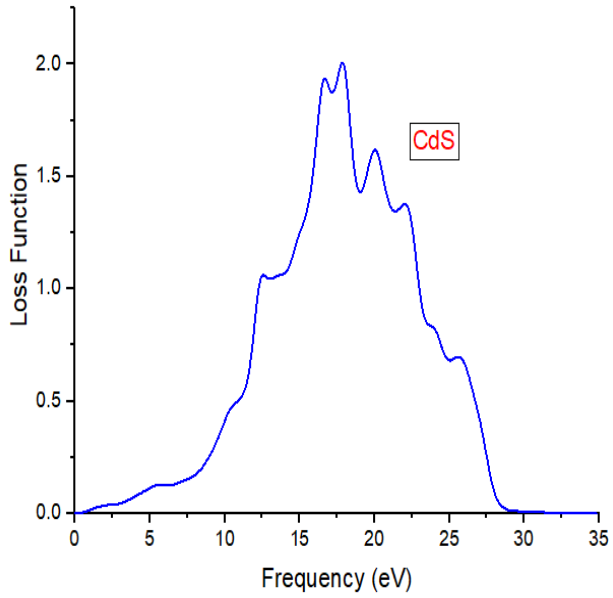

a. CdS

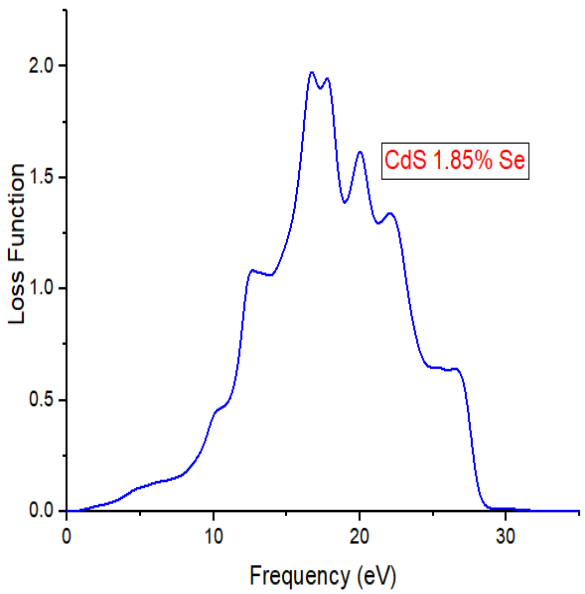

b. CdS 1.85% Se

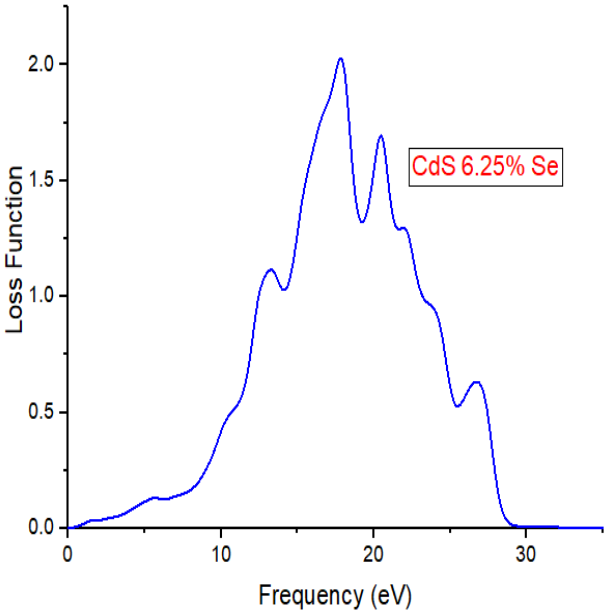

c. CdS 6.25% Se

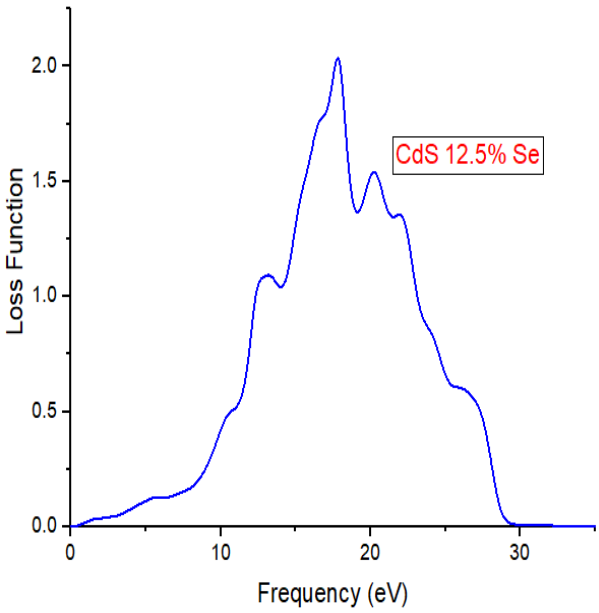

d. CdS 12.5% Se

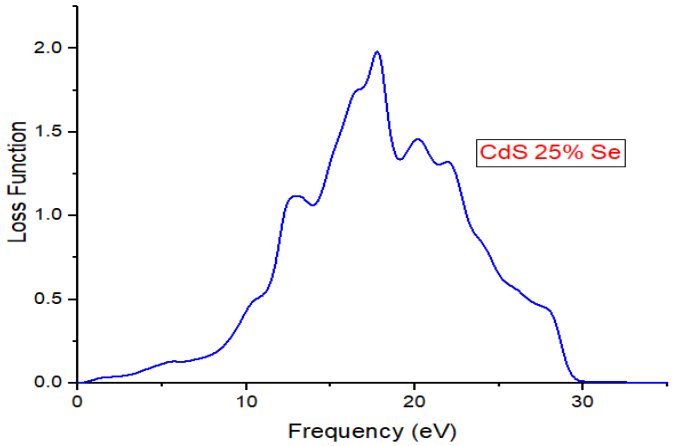

e. CdS 25% Se

Figure 12: Calculated Loss Function for individual pristine CdS and doped Supercells

For pristine CdS (Fig.13 a)) the peak is observed at 17.7eV. Lower peak points are also observed at 13.5eV, 16.5eV, 20eV, 22eV, 25.7eV. The 1.85% Se (Fig.13 b)) doped showed peak at 16.5eV. Other than the peak other lower peaks are also presented at 12.5eV, 20eV, 22eV and 26.5eV. For the 6.25% Se (Fig.13 c)) the peak point is observed at 17.7eV. The graph showed also minor peaks for this concentration at 13.5eV, 20.5eV, 21.5eV and 25.5eV. The 12.5% Se dopant concentration (Fig.13 d)) has a peak at 17.17eV. It has the highest peak compared to all the other supercells. Other lower peaks are also observed at 13eV, 20.3eV and 21.5eV. The highest doped supercell (Fig.13 e)) has the peak point at 17.7eV. Peaks with lower points are observed at 12.7eV, 20.2eV and 21.5eV.

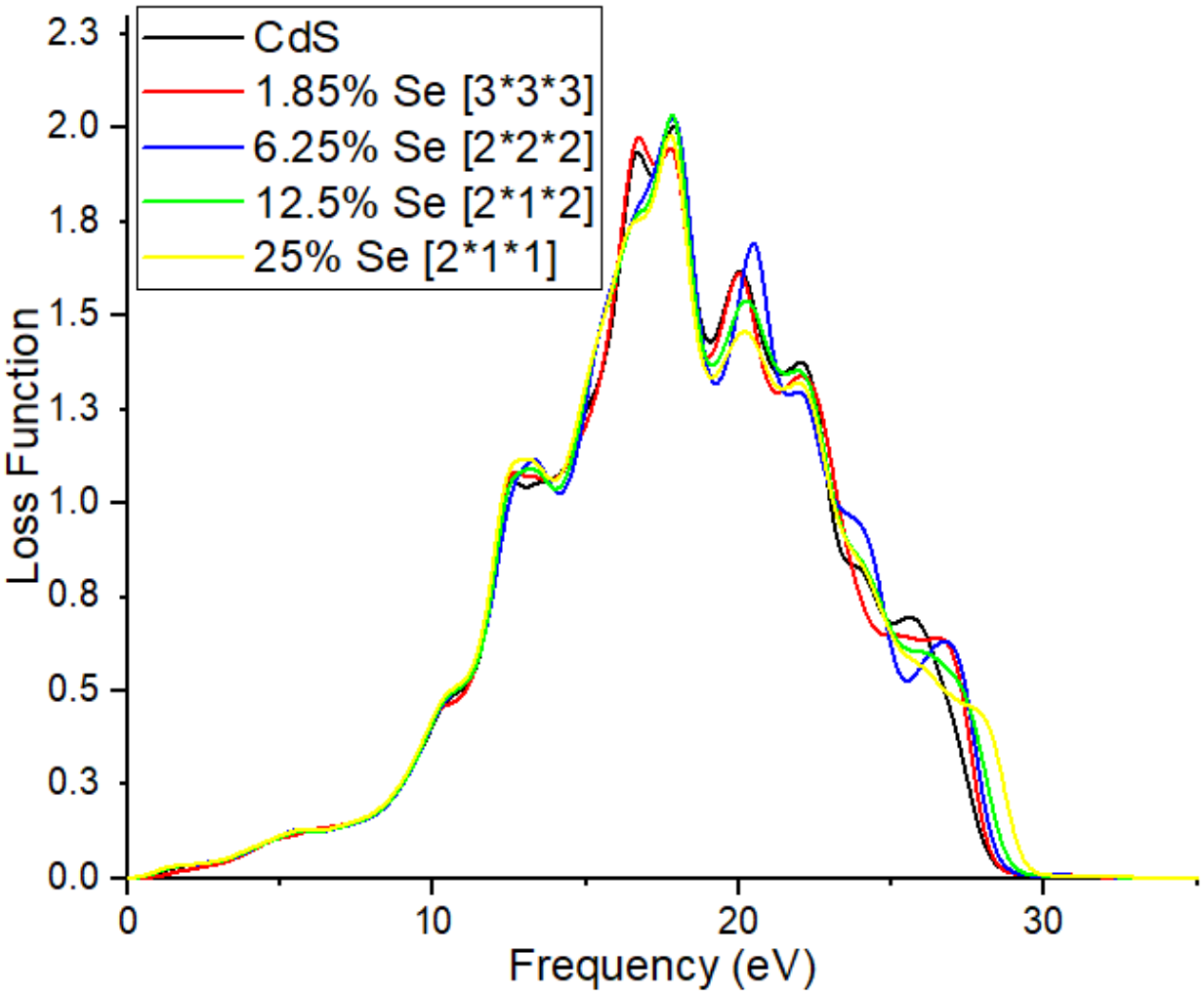

Figure 13: Combined Loss Function

iv. Optical Conductivity

Fig. 13 Illustrates optical conductivity of pristine CdS and doped supercells. For pristine CdS the conductivity is around 6 1/fs but doping the bulk material with Se at concentrations 6.25% and 12.5% is evident that the conductivity increased to 6.2 1/fs. From a broad standpoint, the conductivity characteristics of all Se concentrations are nearly identical. The conductivity characteristic of pure CdS rises at 2.0 eV energy and then abruptly increases until a maximum conductivity is reached at 4.3 eV, after which it drops till 11 eV. After that, there are seven distinct locations where it slowly rises before becoming nearly constant for the remaining higher energy values. For concentrations of Se 1.85%, 6.25%, 12.5%, and 25%, the maximum conductivity is achieved at around 8 eV.

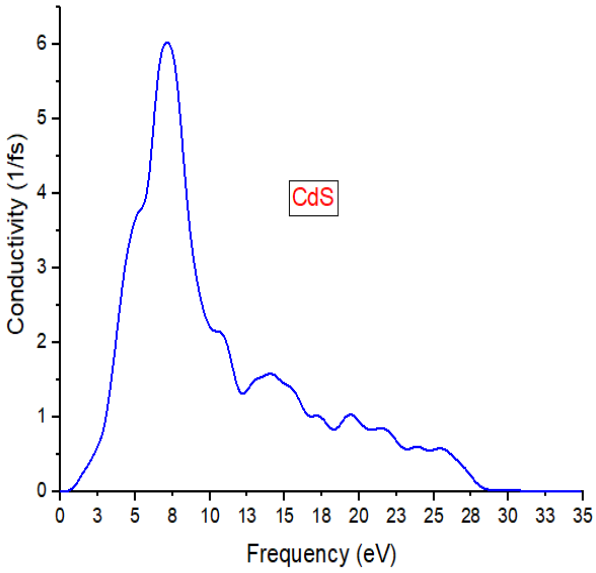

a. CdS

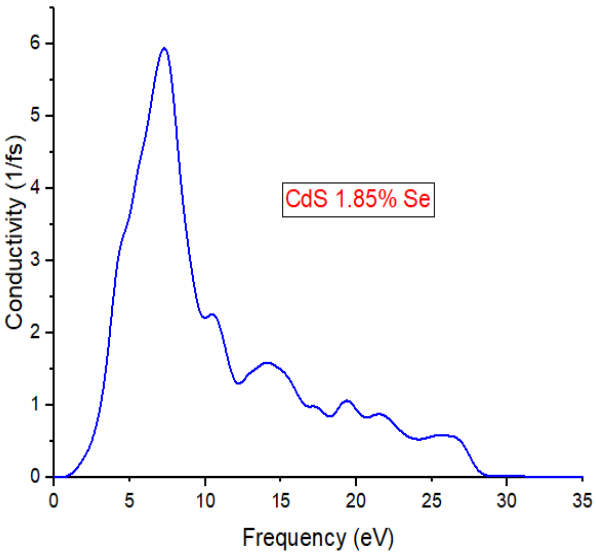

b. CdS 1.85% Se

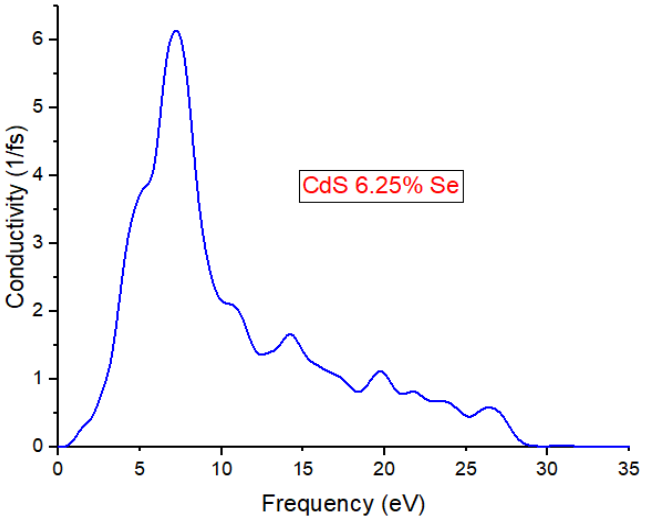

c. CdS 6.25% Se

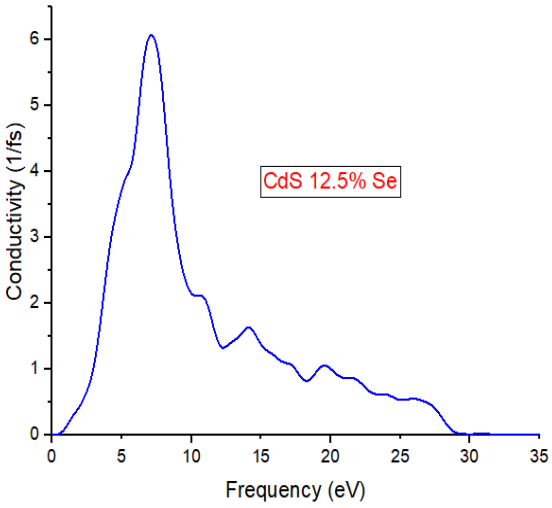

d. CdS 12.5% Se

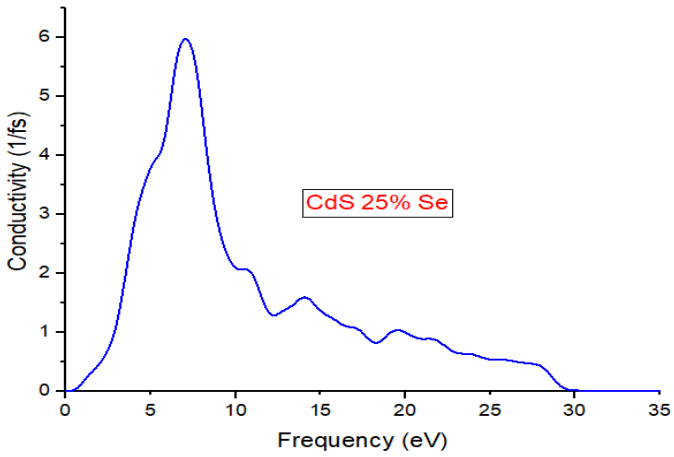

e. CdS 25% Se

Figure 14: Calculated Optical Conductivity for Individual Pristine CdS and doped Supercells

For pristine CdS (Fig.15 a)) the peak optical conductivity is observed at 7.5eV. Lower peak points are also observed at 13.5eV, 18eV, 19.5eV, 21.5eV, 24eV, 25.5eV. The 1.85% Se (Fig.15 b)) doped showed peak at 7.8eV. Other than the peak other lower peaks are also presented at 10.5eV, 14eV, 16.5eV, 19eV, 21.5eV and 26eV. For the 6.25% Se (Fig.15 c)) the peak point is observed at 7.6eV. The graph showed also minor peaks for this concentration at 14eV, 19.8eV, 22eV and 26.5eV. It has the highest peak compared to all the other supercells. The 12.5% Se dopant concentration (Fig.15 d)) has a peak at 7.5eV. Other lower peaks are also observed at 14eV, 19eV and 21eV. The highest doped supercell which is 25% Se (Fig.15 e)) has the peak point at 7.5eV. Peaks with lower points are observed at 14eV, 19eV and 21.5eV. The Zn-doped CdS optical conductivity peak is boosted between 4 and 4.5 eV. There is no improvement in the peak for Al-doped CdS optical conductivity. The region of 0eV to 2eV is where the peak for Na doped CdS optical conductivity is boosted.

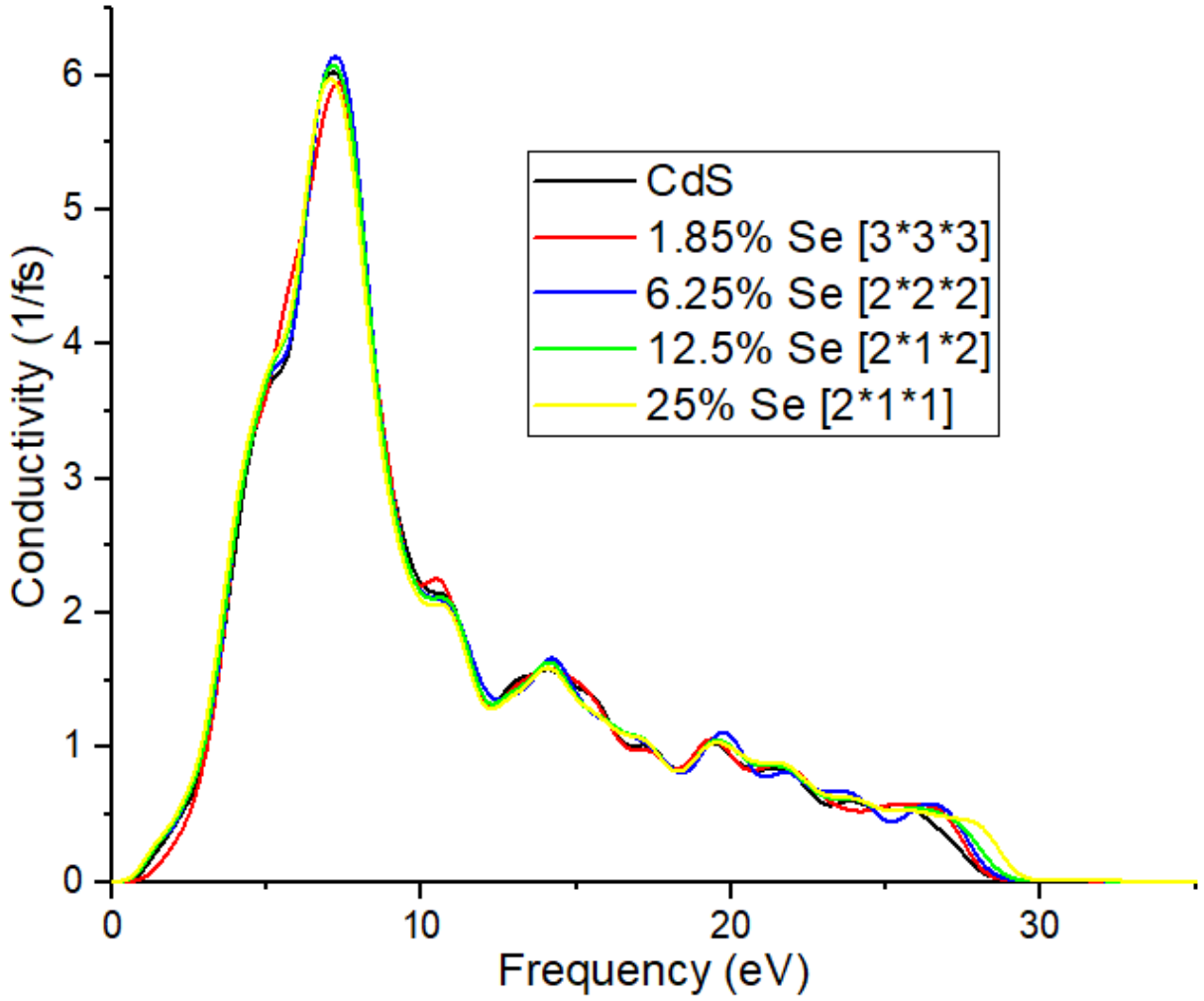

Figure 15: Combined Optical Conductivity

v. Dielectric Function

For the pristine CdS the Dielectric Function peak is at about 7.2 Epsilon but doping increased the peak up to about 7.7 Epsilon. Beginning from 4 eV to 8 eV the Dielectric Function drops from 7.7 Epsilon to -2.2 Epsilon. Again it starts increasing up to 0.5 Epsilon in the Frequency range of 0 to 30 eV. There is a striking resemblance between Figs. 14 and 15. The similarity between dielectric trends and refractive index can be attributed to the lesser values of k2 relative to n2 [81].

It is evident that the dielectric constants found in my DFT analysis are significantly greater than the value of 2.43 that has been measured empirically for pure CdS [14]. In general, the polarization of molecules causes an increase in the dielectric constant of doped materials. The reason for the sharp drop in dielectric constant at high energy (low wavelength) is because polarization does not

keep up with the changing electromagnetic field. In the electronic industry, dielectric constant values of both high and low are crucial. A high dielectric constant is caused by polar groups and intrinsic ions. The materials may find a wide range of uses in the fields of piezoelectric transducers, memory elements, dielectric amplifiers, semiconductor devices, rectifiers, and photonic devices based on capacitors with dielectrics due to the high dielectric constant of the CdS: Se system [82]. Furthermore, CdS: Se material's high dielectric constant makes it possibly suitable for usage in the New Paradigm Super (NPS) capacitors, a new generation of electrostatic capacitors [83].

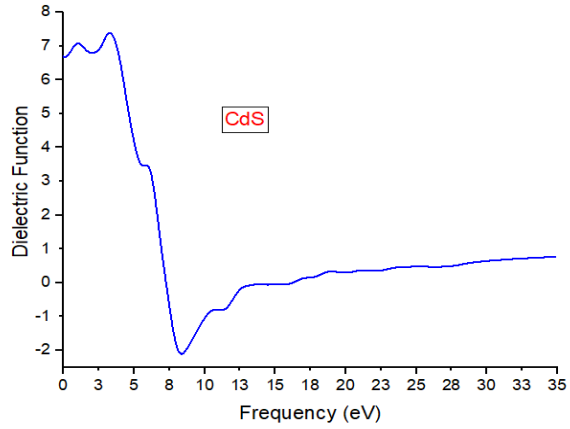

a. CdS

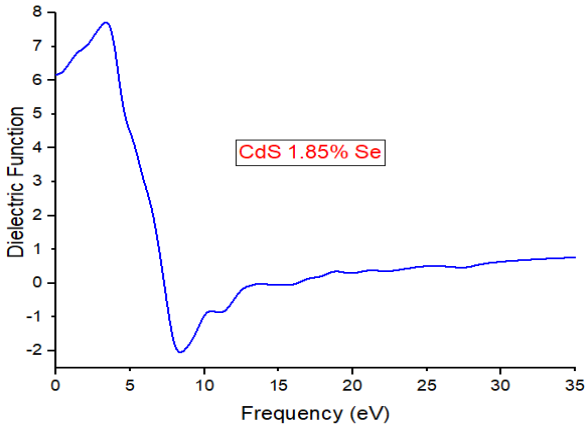

b. CdS 1.85% Se

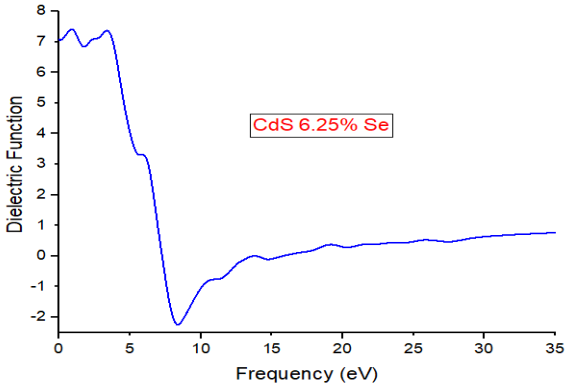

c. CdS 6.25% Se

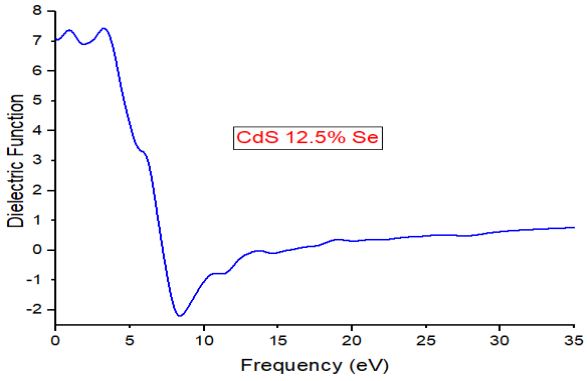

d. CdS 12.5% Se

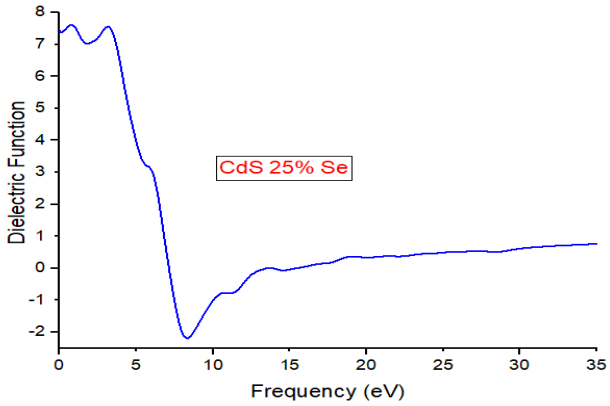

e. CdS 25% Se

Figure 16: Calculated Dielectric Function for individual Pristine CdS and doped Supercells

At 0eV dielectric function of pristine CdS is about 6.7. The highest optical reflectivity at 0eV is observed for 25% Se doped followed by (12.5% and 6.25%) have quite similar values, Pristine CdS and 1.85% doped which have 7.4, 7.1, 6.7 and 6.2 respectively. For the pristine CdS (Fig.17 a)) The peak dielectric function is observed at 3.5eV. Other observed lower peaks are at 1eV, 6eV, 10.5eV, 14eV and 19eV. The 1.85% Se doped (Fig.17 b)) showed peak at 3.5eV. Other lower peaks for this concentration are observed at 6eV, 10.5eV, 14eV and 19eV. The peak dielectric function is observed at 6.25% Se (Fig.17 c)) is at around 1eV and 3.5eV. Lower peaks are also observed at 1eV, 10.5eV, 14eV and 19eV. The 12.5% Se (Fig.17 d)) doped concentration showed peak at 1eV and 3.5eV. Other lower peaks are observed at 1eV, 10.5eV, 14eV and 19eV. For 25% Se doped (Fig.17 e)) the peak is observed at 0.8eV and 3.3eV. Lower peaks are also observed at 10.5eV, 14eV and 19eV. The graph shows the peak dielectric function point for 1.85% Se concentration at 3.5eV. The dielectric function peak for Zn-doped CdS is increased between 4 and 6 eV. Between 0.5 and 1 eV, the peak for the Al-doped CdS dielectric function is strengthened. Between 0 and 0.25 eV, the peak for the Na-doped CdS dielectric function is strengthened.

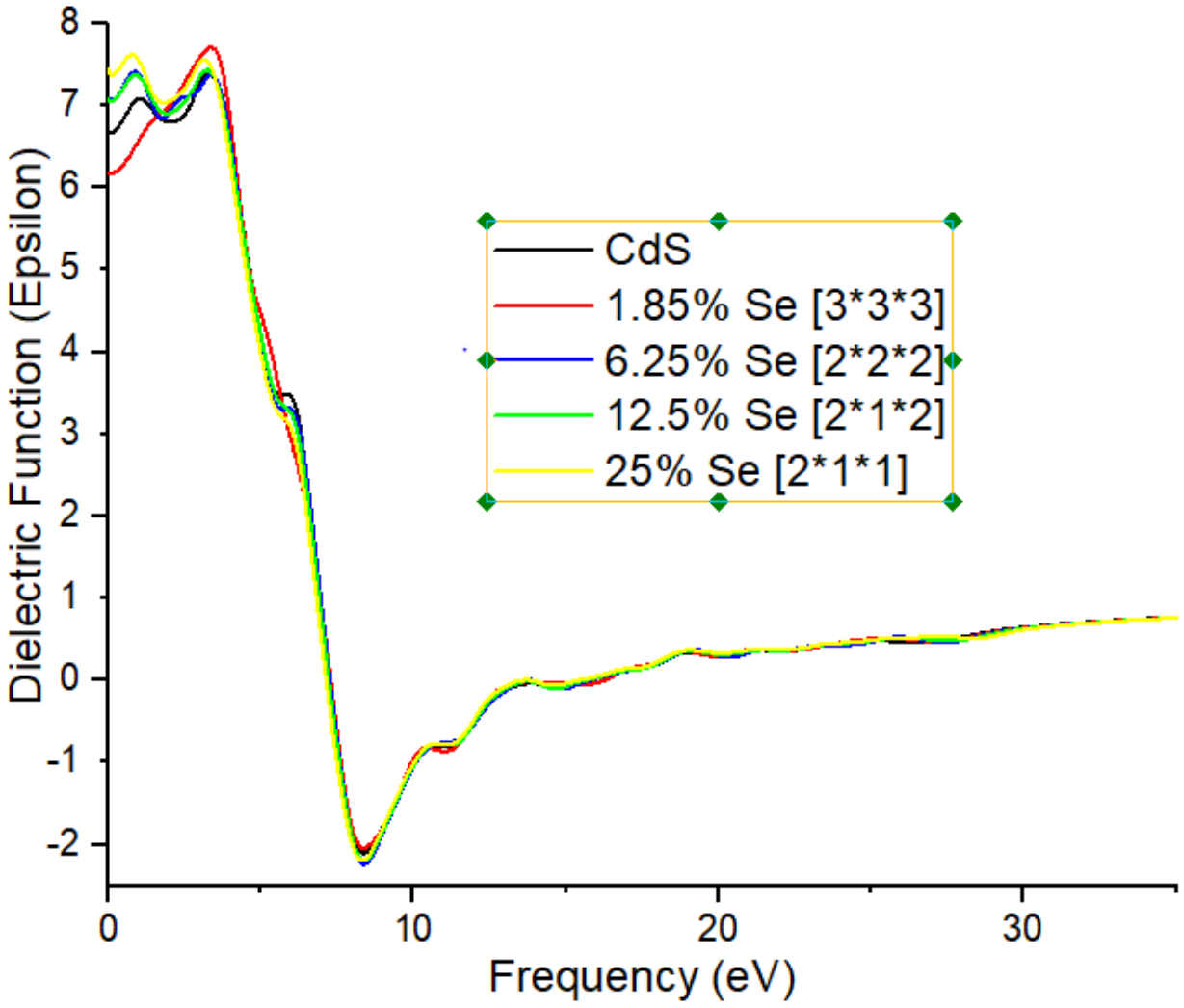

Figure 17: Combined Dielectric Function

vi. Refractive Index

At 0eV refractive index of pristine CdS is about 2.6. The highest optical reflectivity at 0eV is observed for 25% Se doped followed by (12.5% and 6.25%) have quite similar values, Pristine CdS and 1.85% doped which have 2.73, 2.65, 2.6 and 2.45 respectively. For the pristine CdS (Fig.19 a)) The peak dielectric function is observed at 3.5eV. Other observed lower peaks are at 1.5eV, 6.5eV, 13.5eV, 19eV and 51.5eV. The 1.85% Se doped (Fig.19 b)) showed peak at 3.7eV. This concentration as the highest refractive index value. Other lower peaks for this concentration are observed at 10.5eV, 13.5eV, 18.5eV, 21.5eVand 25.5eV. The peak refractive index is observed for 6.25% Se (Fig.19 c)) is at 3.5eV. Lower peaks are also observed at 1.5eV, 6.5eV, 13.5eV and 18.5eV. The 12.5% Se (Fig.19 d)) doped concentration showed peak at 3.5eV. Other lower peaks

are observed at 1.5eV, 13.5eV and 18.5eV. For 25% Se doped (Fig.19 e)) the peak is observed at 3.5eV. Lower peaks are also observed at 1.5eV, 13.5eV and 18.5eV.

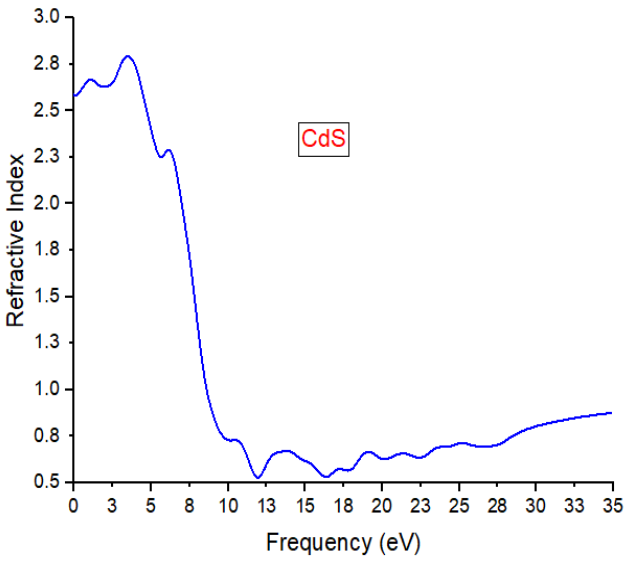

a. CdS

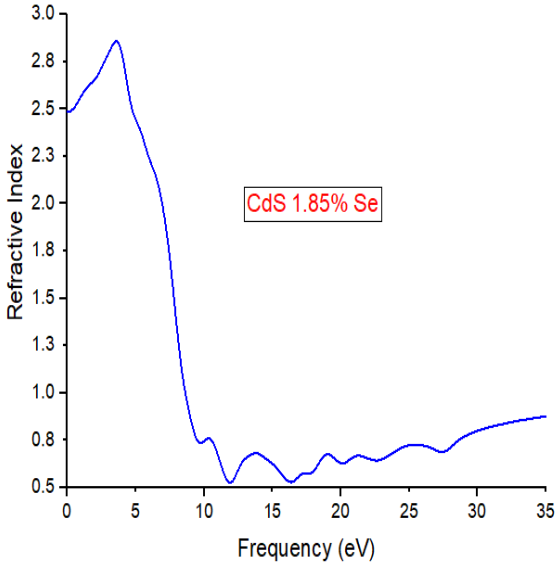

b. CdS 1.85% Se

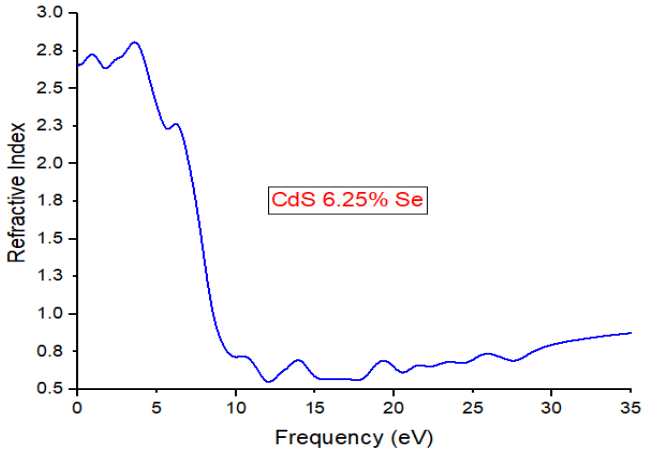

c. CdS 6.25% Se

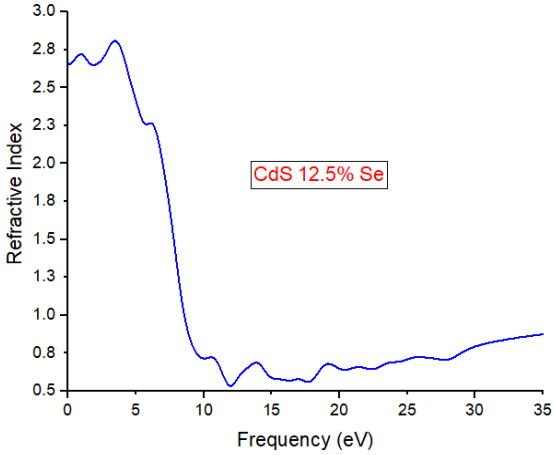

d. CdS 12.5% Se

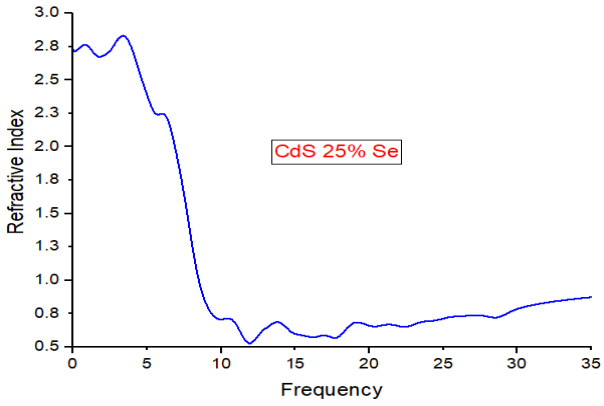

e. CdS 25% Se

Figure 18: Calculated Refractive Index for individual CdS and doped Supercells

The refractive Index peak for the pristine CdS is about 2.82 (arbitrary units) but doping the supercells increased the peak up to about 2.89 to 2.9 (arbitrary units). Experimental value of refractive index for pure CdS thin films is 2.38 at 1.96 eV (˜632.8 nm) [75] [77].

Values of n in the current DFT analysis are greater than the experimental value. The values of n that resulted from DFT calculations at different concentrations of Se during the substitution of Cd atoms with Se atoms in the host CdS lattice are 1.85%, 6.25%, 12.5%, and 25%. However, the refractive index of pure CdS has a DFT value of 2.9. Increases in crystallite size, which result from a decrease in micro-strain, may be associated with higher values of n [84]. According to my DFT analysis, variations in n might be the result of light dispersion when it penetrates the material deeply and interacts successfully with different atoms at varying concentrations of Se. Increased n values for the CdS: Se system might potentially expand its applications in photonics and biomedicine, as well as in the fields of environmental detectors, opthalmics, building displays, anti-reflection coating, solar cells, and photodetectors [85] [86]. According to experimental viewpoints, changes in refractive index might result from a series of internal reflections and could be connected to the cause of photon entrapment by grain boundaries [87] [88]. The Zn-doped CdS refractive index peak is amplified between 4 and 4.5 eV. The Al-doped CdS refractive index peak is amplified between 0.5 and 1 eV. The Na-doped CdS refractive index peak is strengthened between 0 and 0.5 eV.

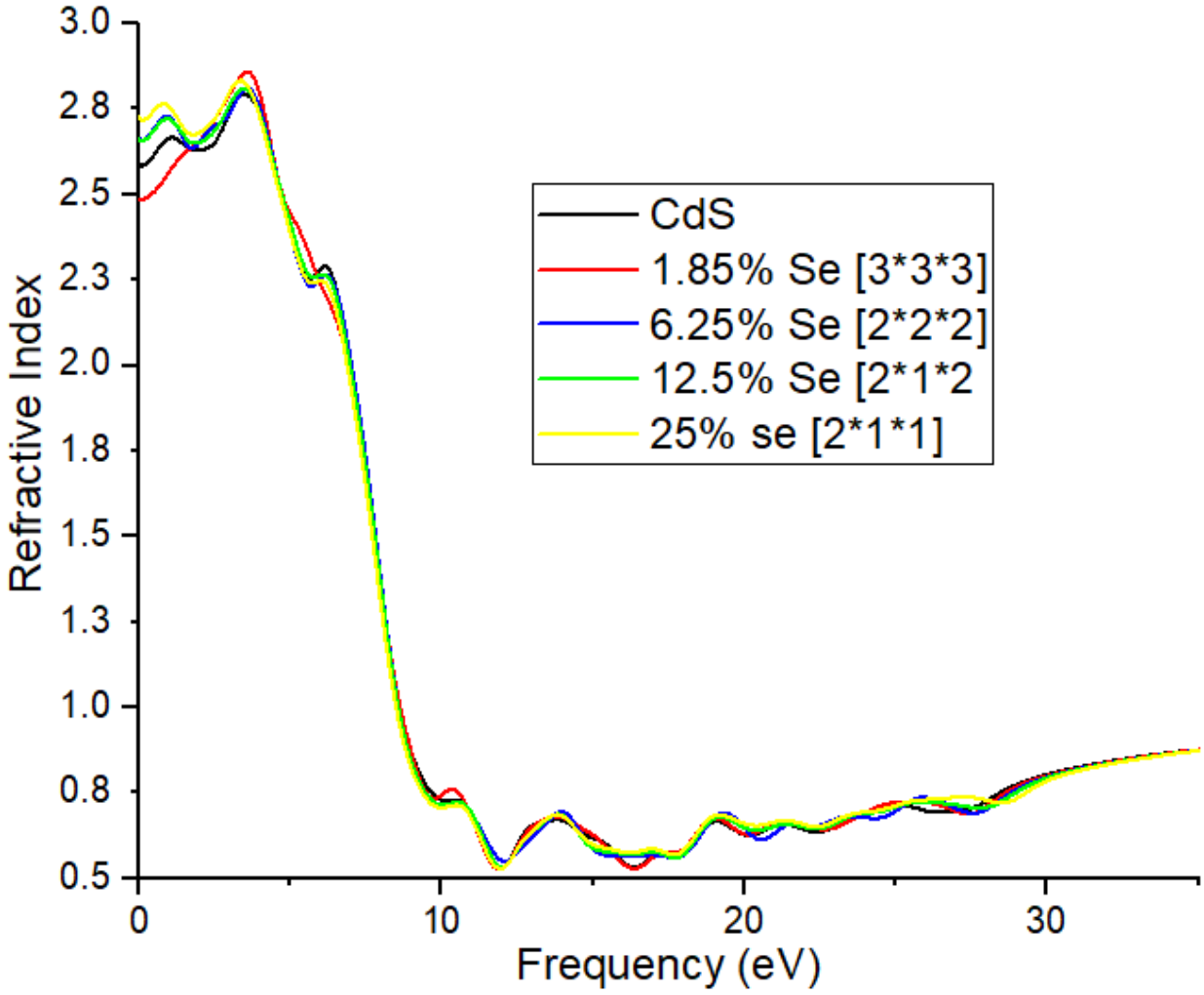

Figure 19: Combined Refractive Index

CHAPTER FIVE

CONCLUSION

This research used DFT calculations to calculate the electrical and optical properties of pristine CdS and four other created supercells. The supercells are (2 X 1 X 1), (2 X 1 X 2), (2 X 2 X 2) and (3 X 3 X 3) which are 25%, 12.5%, 6.25% and 1.85% Se doped respectively.

The DFT calculations revealed that doping CdS with Se significantly decreased the band-gap. The research also enabled me to calculate different optical properties such as absorption, reflectivity, conductivity, loss function, refractive index and dielectric function. From the DFT result I found out that the optical properties are improved with doping. The optical absorption is highest at the doping concentration of 6.25% of Se at 8eV. At this concentration it is possible if we use it for solar cell and photo detector applications. For optical reflectivity, the peak at 0eV is observed for 25% doping concentration of Se but at 8eV; I found the peak reflectivity for 6.25% Se. The peak loss function occurred at 12.5% Se at 17.17eV. The compound showed highest conductivity at 6.25% Se at 7.6eV followed by 12.5% Se. The peak dielectric function is observed at the dopant concentration of 1.85% at 3.5eV. The second highest point is for 12.5% Se concentration. The refractive index also has the highest value at 1.85% Se at 3.7eV followed by 25% Se.

Decreased bandgap will make the material to have potential applications in Solar cells, Organic thin-film transistors, Corrosion control coatings and Near-infrared (NIR) photodetectors. Improved optical properties will enable the doped materials to have applications in lasers, light-emitting diodes, and solar cells.

In conclusion, doping Cadmium Sulfide with selenium has decreased the band-gap as well as improved the optical properties. These doped materials will have increased applications as optoelectronics.

FUTURE WORK

Bulk CdS material doped with selenium (Se) is used in this study to investigate its potential for photocatalytic uses. The results show that the doping improves the material's charge carrier dynamics and light absorption capabilities. By examining two-dimensional (2D) CdS doped with Se, future researchers can expand on this study and potentially provide increased surface area and catalytic efficiency for water splitting applications. Significant improvements in photocatalytic processes, which would make them more sustainable and effective for producing hydrogen, might result from the switch to 2D materials. In the upcoming years, such developments may significantly affect renewable energy technology.

REFERENCES

[1] M. Isshiki and J. Wang, “Wide-bandgap ii-vi semiconductors: growth and properties,” *Springer Handbooks*, p. 1, 2017, doi: 10.1007/978-3-319-48933-9_16.

[2] A. S. Z. Lahewil, Y. Al-Douri, U. Hashim, and N. M. Ahmed, “Structural, analysis and optical studies of cadmium sulfide nanostructured,” *Procedia Eng.*, vol. 53, pp. 217–224, 2013, doi: 10.1016/j.proeng.2013.02.029.

[3] M. Junaid Iqbal Khan, M. N. Usmani, and Z. Kanwal, “Novel optical properties of CdS:Zn rocksalt system (a theoretical study),” *Mater. Res. Express*, vol. 4, no. 11, 2017, doi: 10.1088/2053-1591/aa93c4.

[4] J. Frenzel, “Structural, electronic and optical properties of cadmium sulfide nanoparticles,” *Thesis*, no. May, p. 135, 2007.

[5] R. Banerjee, R. Jayakrishnan, and P. Ayyub, “Effect of the size-induced structural transformation on the band gap in CdS nanoparticles,” *J. Phys. Condens. Matter*, vol. 12, no. 50, pp. 10647–10654, 2000, doi: 10.1088/0953-8984/12/50/325.

[6] Y. K. Liu *et al.*, “High-quality CdS nanoribbons with lasing cavity,” *Appl. Phys. Lett.*, vol. 85, no. 15, pp. 3241–3243, 2004, doi: 10.1063/1.1805714.

[7] A. Majid, R. Ahmad, A. Nabi, A. Shakoor, and N. Hassan, “A density functional theory study of Raman modes of hydrogenated cadmium sulphide nanoparticles,” *Nanomater. Nanotechnol.*, vol. 2, no. 1, pp. 2–9, 2012, doi: 10.5772/51565.

[8] N. Ali, M. A. Iqbal, S. T. Hussain, M. Waris, and S. A. Munair, “Optoelectronic properties of cadmium sulfide thin films deposited by thermal evaporation technique,” *Key Eng. Mater.*, vol. 510–511, no. 1, pp. 177–185, 2012, doi:

10.4028/www.scientific.net/KEM.510-511.177.

[9] M. Seol, H. Kim, W. Kim, and K. Yong, “Highly efficient photoelectrochemical hydrogen generation using a ZnO nanowire array and a CdSe/CdS co-sensitizer,” *Electrochem. commun.*, vol. 12, no. 10, pp. 1416–1418, 2010, doi: 10.1016/j.elecom.2010.07.035.

[10] O. P. Dimitriev, V. V. Kislyuk, A. F. Syngaevsky, P. S. Smertenko, and A. A. Pud, “Different roles of cadmium-and sulfur (selenium)-terminated crystal facets in the formation of a photovoltaic response from hybrid organic/inorganic CdS (CdSe) heterojunctions,” *Phys. Status Solidi Appl. Mater. Sci.*, vol. 206, no. 11, pp. 2645–2651, 2009, doi: 10.1002/pssa.200925143.

[11] S. P. Mondal and S. K. Ray, “Cadmium sulfide nanostructures for photovoltaic devices,” *Proc. Natl. Acad. Sci. India Sect. A - Phys. Sci.*, vol. 82, no. 1, pp. 21–29, 2012, doi: 10.1007/s40010-012-0002-3.

[12] J. Even *et al.*, “Density functional theory simulations of semiconductors for photovoltaic applications: Hybrid organic-inorganic perovskites and III/V heterostructures,” *Int. J. Photoenergy*, vol. 2014, 2014, doi: 10.1155/2014/649408.

[13] M. Sahakyan and V. H. Tran, “Density functional theory study of electronic structure and optical properties of YGa2,” *Comput. Mater. Sci.*, vol. 184, no. February, p. 109898, 2020, doi: 10.1016/j.commatsci.2020.109898.

[14] P. Li *et al.*, “First-principle study of optical properties of Cu-doped CdS,” *Opt. Commun.*, vol. 295, pp. 45–52, 2013, doi: 10.1016/j.optcom.2012.12.086.

[15] L. Dhatchinamurthy, P. Thirumoorthy, L. Arunraja, and S. Karthikeyan, “Synthesis and

characterization of cadmium sulfide (CdS) thin film for solar cell applications grown by dip coating method," *Mater. Today Proc.*, vol. 26, no. xxxx, pp. 3595–3599, 2019, doi: 10.1016/j.matpr.2019.08.219.

[16] M. Eskandari, V. Ahmadi, and R. Ghahary, "Enhanced photovoltaic performance of a cadmium sulfide/cadmium selenide-sensitized solar cell using an aluminum-doped zinc oxide electrode," *Ceram. Int.*, vol. 41, no. 2, pp. 2373–2380, 2015, doi: 10.1016/j.ceramint.2014.10.051.

[17] M. J. I. Khan and Z. Kanwal, "First principle calculations of optical properties of CdS:Al system (A DFT + U study)," *Mater. Res. Express*, vol. 6, no. 3, 2019, doi: 10.1088/2053-1591/aaf5a8.

[18] M. Shishkin and G. Kresse, "Implementation and performance of the frequency-dependent GW method within the PAW framework," *Phys. Rev. B - Condens. Matter Mater. Phys.*, vol. 74, no. 3, pp. 1–13, 2006, doi: 10.1103/PhysRevB.74.035101.

[19] C. Freysoldt *et al.*, "First-principles calculations for point defects in solids," *Rev. Mod. Phys.*, vol. 86, no. 1, pp. 253–305, 2014, doi: 10.1103/RevModPhys.86.253.

[20] S. H. Wei and A. Zunger, "Calculated natural band offsets of all II-VI and III-V semiconductors: Chemical trends and the role of cation d orbitals," *Appl. Phys. Lett.*, vol. 72, no. 16, pp. 2011–2013, 1998, doi: 10.1063/1.121249.

[21] B. Radisavljevic, A. Radenovic, J. Brivio, V. Giacometti, and A. Kis, "Single-layer MoS2 transistors," *Nat. Nanotechnol.*, vol. 6, no. 3, pp. 147–150, 2011, doi: 10.1038/nnano.2010.279.

[22] M. S. Hybertsen and S. G. Louie, “Electron correlation in semiconductors and insulators: Band gaps and quasiparticle energies,” *Phys. Rev. B*, vol. 34, no. 8, pp. 5390–5413, 1986, doi: 10.1103/PhysRevB.34.5390.

[23] A. Slonopas *et al.*, “Growth mechanisms and their effects on the opto-electrical properties of CdS thin films prepared by chemical bath deposition,” *Mater. Sci. Semicond. Process.*, vol. 52, pp. 24–31, 2016, doi: 10.1016/j.mssp.2016.05.011.

[24] G. Sasikala, P. Thilakan, and C. Subramanian, “Modification in the chemical bath deposition apparatus, growth and characterization of CdS semiconducting thin films for photovoltaic applications,” *Sol. Energy Mater. Sol. Cells*, vol. 62, no. 3, pp. 275–293, 2000, doi: 10.1016/S0927-0248(99)00170-1.

[25] S. U. Shaikh *et al.*, “Effects of air annealing on CdS quantum dots thin film grown at room temperature by CBD technique intended for photosensor applications,” *Mater. Res. Bull.*, vol. 47, no. 11, pp. 3440–3444, 2012, doi: 10.1016/j.materresbull.2012.07.009.

[26] W. Zhao *et al.*, “Single CdS Nanorod for High Responsivity UV–Visible Photodetector,” *Adv. Opt. Mater.*, vol. 5, no. 12, pp. 1–7, 2017, doi: 10.1002/adom.201700159.

[27] Z. Makhdoumi-Kakhaki, A. Youzbashi, P. Sangpour, N. Naderi, and A. Kazemzadeh, “Effects of film thickness and stoichiometric on the electrical, optical and photodetector properties of CdS quantum dots thin films deposited by chemically bath deposition method at different bath temperature,” *J. Mater. Sci. Mater. Electron.*, vol. 27, no. 12, pp. 12931–12939, 2016, doi: 10.1007/s10854-016-5430-4.

[28] Y. Li *et al.*, “Fabrication and electrical properties of (0 0 2)-oriented grown CdS/Si heterojunctions by radio frequency magnetron sputtering,” *Mater. Lett.*, vol. 228, pp. 463–

465, 2018, doi: 10.1016/j.matlet.2018.06.096.

[29] M. Tomakin, M. Altunbaş, E. Bacaksiz, and Ş. Çelik, "Current transport mechanism in CdS thin films prepared by vacuum evaporation method at substrate temperatures below room temperature," *Thin Solid Films*, vol. 520, no. 7, pp. 2532–2536, 2012, doi: 10.1016/j.tsf.2011.10.160.

[30] M. M. Rahman, M. M. Alam, and A. M. Asiri, "Potential application of mixed metal oxide nanoparticle-embedded glassy carbon electrode as a selective 1,4-dioxane chemical sensor probe by an electrochemical approach," *RSC Adv.*, vol. 9, no. 72, pp. 42050–42061, 2019, doi: 10.1039/c9ra09118a.

[31] U. Abdullah, M. Ali, and E. Pervaiz, "An Inclusive Review on Recent Advancements of Cadmium Sulfide Nanostructures and its Hybrids for Photocatalytic and Electrocatalytic Applications," *Mol. Catal.*, vol. 508, no. April, p. 111575, 2021, doi: 10.1016/j.mcat.2021.111575.

[32] M. Z. Ghori *et al.*, "Role of UV Plasmonics in the Photocatalytic Performance of TiO2 Decorated with Aluminum Nanoparticles," *ACS Appl. Nano Mater.*, vol. 1, no. 8, pp. 3760–3764, 2018, doi: 10.1021/acsanm.8b00853.

[33] Z. R. Tang, B. Han, C. Han, and Y. J. Xu, "One dimensional CdS based materials for artificial photoredox reactions," *J. Mater. Chem. A*, vol. 5, no. 6, pp. 2387–2410, 2017, doi: 10.1039/C6TA06373J.

[34] B. Y. Xia *et al.*, "One-Dimensional Nanostructures : Synthesis , Characterization , and Applications **," no. 5, pp. 353–389, 2003.

[35] G.W.A.D., *Solid state electronic devices*, vol. 12, no. 1. 1973. doi: 10.1016/0026-2714(73)90713-0.

[36] D. Neamen, *Semiconductors Physics and Devices*. 2011.

[37] S. Lany, “Semiconductor thermochemistry in density functional calculations,” *Phys. Rev. B - Condens. Matter Mater. Phys.*, vol. 78, no. 24, pp. 1–8, 2008, doi: 10.1103/PhysRevB.78.245207.

[38] G. Commentary, “Semiconductor Photocatalysis Past, Present, and Future Outlook,” 2012.

[39] E. F. Schubert, “Light-emitting diodes,” 1993.

[40] J. Van Vechten, “Quantum dielectric theory of electronegativity in covalent systems. I. Electronic dielectric constant,” *Phys. Rev.*, vol. 182, no. 3, pp. 891–905, 1969, [Online]. Available: http://prola.aps.org/abstract/PR/v182/i3/p891_1

[41] K. K. N. S.M.Sze, *Physics of Semiconductor Devices Physics of Semiconductor Devices*, vol. 10. 1995.

[42] M. R. Hoffmann, S. T. Martin, W. Choi, and D. W. Bahnemann, “Environmental Applications of Semiconductor Photocatalysis,” *Chem. Rev.*, vol. 95, no. 1, pp. 69–96, 1995, doi: 10.1021/cr00033a004.

[43] M. J. Iqbal Khan and Z. Kanwal, “Investigation of optical properties of CdS for various Na concentrations for nonlinear optical applications (A DFT study),” *Optik (Stuttg).*, vol. 193, no. April, 2019, doi: 10.1016/j.ijleo.2019.162985.

[44] W. Saoca and / Ay, “TA-4-a77OAPAWAY,” vol. 25, p. 347, 1951.

[45] H. Kroemer, “Kroemer-Lecture,” 2000.

[46] F. Capasso, “Band-Gap Engineering: From Physics and Materials To New Semiconductor Devices.,” *Science (80-.).*, vol. 235, no. 4785, pp. 172–176, 1987, doi: 10.1126/science.235.4785.172.

[47] H. Kroemer, “Quasi-Electric Fields and Band Offsets: Teaching Electrons New Tricks,” *Sel. Work. Profr. Herbert Kroemer*, vol. 73, no. July, pp. 22–42, 2008, doi: 10.1142/9789812709028_0004.

[48] P. Hautojärvi and A. Vehanen, *Positrons in Solids; Topics in Current Physics*, vol. 173, no. Part_1. 1979. [Online]. Available: http://www.degruyter.com/doi/10.1524/zpch.1991.173.Part_1.125

[49] K. Hess, “emission of phonons may become exceedingly impor-,” vol. 34, pp. 3–6, 1980.

[50] TSU LESAKIR, “Superlattice and Negative Differential Conductivity in Semiconductor,” *IBM J. Res. Dev.*, vol. 14, no. 1, pp. 61–65, 1970, doi: 10.1147/rd.141.0061.

[51] B. Mishra and P. Hazarika, “Rare greenockite (CdS) within the chromite-PGE association in the Bangur Gabbro, Baula-Nuasahi Complex, Eastern India,” *Ore Geol. Rev.*, vol. 72, pp. 1327–1334, 2016, doi: 10.1016/j.oregeorev.2015.04.006.

[52] E. D. Palik, *Handbook of optical constants of solids*, vol. 1. 2012. doi: 10.1016/C2009-0-20920-2.

[53] T. I. Alanazi, R. A. Alenazi, and A. M. El Sayed, “Tuning the band gap, optical, mechanical, and electrical features of a bio-blend by Cr2O3/V2O5 nanofillers for optoelectronics and energy applications,” *Sci. Rep.*, vol. 14, no. 1, pp. 1–17, 2024, doi:

10.1038/s41598-024-62643-6.

[54] M. B. Pramanik, M. A. Al Rakib, M. A. Siddik, and S. Bhuiyan, “Doping Effects and Relationship between Energy Band Gaps, Impact of Ionization Coefficient and Light Absorption Coefficient in Semiconductors,” *Eur. J. Eng. Technol. Res.*, vol. 9, no. 1, pp. 10–15, 2024, doi: 10.24018/ejeng.2024.9.1.3118.

[55] A. Biswas, S. R. Meher, and D. K. Kaushik, “Electronic and Band Structure calculation of Wurtzite CdS Using GGA and GGA+U functionals,” *J. Phys. Conf. Ser.*, vol. 2267, no. 1, 2022, doi: 10.1088/1742-6596/2267/1/012155.

[56] P. Khatri and M. N. Huda, “Application of attractive potential by DFT + U to predict the electronic properties of materials without highly localized bands,” *Comput. Mater. Sci.*, vol. 81, pp. 290–295, 2014, doi: 10.1016/j.commatsci.2013.08.031.

[57] M. Junaid Iqbal Khan, Z. Kanwal, M. Nauman Usmani, M. Yousef, P. Akhtar, and A. Nabi, “Effect of Ni concentration on optical properties of rocksalt CdS system (A DFT + U study),” *Int. J. Mod. Phys. B*, vol. 32, no. 25, pp. 1–19, 2018, doi: 10.1142/S0217979218502806.

[58] U. Pal, R. Silva-González, G. Martínez-Montes, M. Gracia-Jiménez, M. A. Vidal, and S. Torres, “Optical characterization of vacuum evaporated cadmium sulfide films,” *Thin Solid Films*, vol. 305, no. 1–2, pp. 345–350, 1997, doi: 10.1016/S0040-6090(97)00124-7.

[59] B. K. Sarkar, “Ab-Initio Calculations of Structural, Electronic, and Optical Properties of Cd1–xMnxTeAb-Initio Calculations of Structural, Electronic, and Optical Properties of Cd1–xMnxTe,” *Int. J. Appl. Phys. Math.*, vol. 4, no. 3, pp. 176–179, 2014, doi: 10.7763/ijapm.2014.v4.278.

[60] R. Sathyamoorthy *et al.*, "Surfactant-assisted synthesis of Cd1-xCoxS nanocluster alloys and their structural, optical and magnetic properties," *J. Alloys Compd.*, vol. 493, no. 1–2, pp. 240–245, 2010, doi: 10.1016/j.jallcom.2009.12.063.

[61] P. A. N. C. N. U. P. E. Agbo F. U. Nweke, "Effects of Concentration on the Properties of Zn-doped Cadmium Sulphide Thin Films," *Int. J. Sci. Res.*, vol. 3, no. 11, p. —, 2014, [Online]. Available: https://www.researchgate.net/profile/Patrick-Nwofe/publication/268522310_Effectsof_Concentration_on_the_Propertiesof_Zn-doped_Cadmium_Sulphide_Thin_Films/links/546f84d00cf24af340c08faf/Effectsof-Concentration-on-the-Propertiesof-Zn-doped-Cadmium-Sulphide-

[62] S. Chandramohan, A. Kanjilal, S. N. Sarangi, S. Majumder, R. Sathyamoorthy, and T. Som, "Effect of Fe-ion implantation doping on structural and optical properties of CdS thin films," *Appl. Phys. A Mater. Sci. Process.*, vol. 99, no. 4, pp. 837–842, 2010, doi: 10.1007/s00339-010-5598-z.

[63] M. Anbarasi, V. S. Nagarethinam, and A. R. Balu, "Investigations on the structural, morphological, optical and electrical properties of undoped and nanosized Zn-doped CdS thin films prepared by a simplified spray technique," *Mater. Sci. Pol.*, vol. 32, no. 4, pp. 652–660, 2014, doi: 10.2478/s13536-014-0244-7.

[64] K. Lakshmy, E. B. Rincy, and J. M. T. V Vimalkumar, "Optoelectronic properties of Zn-doped and air- annealed CdS thin film for Photovoltaic applications," *Int. Res. J. Eng. Technol.*, pp. 437–441, 2015.

[65] F. Yang, N. N. Yan, S. Huang, Q. Sun, L. Z. Zhang, and Y. Yu, "Zn-doped CdS nanoarchitectures prepared by hydrothermal synthesis: Mechanism for enhanced

photocatalytic activity and stability under visible light," *J. Phys. Chem. C*, vol. 116, no. 16, pp. 9078–9084, 2012, doi: 10.1021/jp300939q.

[66] L. A. Wessjohann, A. Schneider, M. Abbas, and W. Brandt, "Selenium in chemistry and biochemistry in comparison to sulfur," *Biol. Chem.*, vol. 388, no. 10, pp. 997–1006, 2007, doi: 10.1515/BC.2007.138.

[67] R. A. Vargas-Hernández, "Bayesian Optimization for Calibrating and Selecting Hybrid-Density Functional Models," *J. Phys. Chem. A*, vol. 124, no. 20, pp. 4053–4061, 2020, doi: 10.1021/acs.jpca.0c01375.

[68] J. D. Pack and H. J. Monkhorst, "'special points for Brillouin-zone integrations'-a reply," *Phys. Rev. B*, vol. 16, no. 4, pp. 1748–1749, 1977, doi: 10.1103/PhysRevB.16.1748.

[69] P. Giannozzi *et al.*, "QUANTUM ESPRESSO: A modular and open-source software project for quantum simulations of materials," *J. Phys. Condens. Matter*, vol. 21, no. 39, 2009, doi: 10.1088/0953-8984/21/39/395502.

[70] T. G. Edossa and M. M. Woldemariam, "Electronic, Structural, and Optical Properties of Zinc Blende and Wurtzite Cadmium Sulfide (CdS) Using Density Functional Theory," *Adv. Condens. Matter Phys.*, vol. 2020, 2020, doi: 10.1155/2020/4693654.

[71] A. I. Sidorov, A. V. Nashchekin, R. A. Castro, I. N. Anfimova, and T. V. Antropova, "Optical and dielectric properties of nanocomposites on base nanoporous glasses with silver and silver iodide nanowires," *Phys. B Condens. Matter*, vol. 603, p. 412764, 2021, doi: 10.1016/j.physb.2020.412764.

[72] G. Cerchiari, S. Erlewein, P. Yzombard, M. Zimmermann, and A. Kellerbauer, "Ac ce pte

us cri," *J. Phys. B At. Mol. Opt. Phys.*, pp. 0–14, 2019.

[73] W. Kohn, "Density functional and density matrix method scaling linearly with the number of atoms," *Phys. Rev. Lett.*, vol. 76, no. 17, pp. 3168–3171, 1996, doi: 10.1103/PhysRevLett.76.3168.

[74] E. Esakkiraj *et al.*, "Optostructral and vibrational characteristics of Cu:CdS nanoparticles by precipitation method," *Optik (Stuttg).*, vol. 124, no. 21, pp. 5229–5231, 2013, doi: 10.1016/j.ijleo.2013.04.003.

[75] M. J. I. Khan *et al.*, "Theoretical studies of optical properties of Cu doped rocksalt CdS," *J. Alloys Compd.*, vol. 695, pp. 3605–3611, 2017, doi: 10.1016/j.jallcom.2016.11.402.

[76] J. Hasanzadeh and S. F. Shayesteh, "Luminescence of doped CdS nanocrystals: Effect of doping and capping agent," *Opt. Appl.*, vol. 41, no. 4, pp. 921–928, 2011.

[77] M. J. I. Khan, Z. Kanwal, M. N. Usmani, M. Zeeshan, and M. Yousaf, "An insight into optical properties of Pb:CdS system (a theoretical study)," *Mater. Res. Express*, vol. 6, no. 6, 2019, doi: 10.1088/2053-1591/ab0abf.

[78] W. Benstaali, S. Bentata, H. A. Bentounes, A. Abbad, and B. Bouadjemi, "Influence of Ni-Ni separation on the optoelectronic and magnetic properties of Ni-doped cubic cadmium sulphide," *Mater. Sci. Semicond. Process.*, vol. 17, pp. 53–58, 2014, doi: 10.1016/j.mssp.2013.08.007.

[79] M. Junaid Iqbal Khan, Z. Kanwal, M. Nauman Usmani, P. Akhtar, A. Nabi, and N. Ahmad, "Optical changes in rock-salt CdS system under increasing silver concentrations effects," *Acta Phys. Pol. A*, vol. 134, no. 6, pp. 1099–1107, 2018, doi:

10.12693/APhysPolA.134.1099.

[80] B. Bhattacharya and U. Sarkar, “The effect of boron and nitrogen doping in electronic, magnetic, and optical properties of graphyne,” *J. Phys. Chem. C*, vol. 120, no. 47, pp. 26793–26806, 2016, doi: 10.1021/acs.jpcc.6b07478.

[81] H. S. AL-Jumaili, “Structural and Optical Properties of Nanocrystalline Pb1-xCdxS Thin Films Prepared by Chemical Bath Deposition,” *Appl. Phys. Res.*, vol. 4, no. 3, pp. 75–82, 2012, doi: 10.5539/apr.v4n3p75.

[82] B. Zhao *et al.*, “A versatile foaming platform to fabricate polymer/carbon composites with high dielectric permittivity and ultra-low dielectric loss,” *J. Mater. Chem. A*, vol. 7, no. 1, pp. 133–140, 2019, doi: 10.1039/c8ta05556d.

[83] S. Fromille and J. Phillips, “Super dielectric materials,” *Materials (Basel).*, vol. 7, no. 12, pp. 8197–8212, 2014, doi: 10.3390/ma7128197.

[84] R. Premarani, J. Jebaraj Devadasan, S. Saravanakumar, R. Chandramohan, and T. Mahalingam, “Structural, optical and magnetic properties of Ni-doped CdS thin films prepared by CBD,” *J. Mater. Sci. Mater. Electron.*, vol. 26, no. 4, pp. 2059–2065, 2015, doi: 10.1007/s10854-014-2647-y.

[85] T. Neubert and M. Vergöhl, “Optical Thin Films and Coatings,” *Opt. Thin Film. Coatings*, no. June 2018, pp. 427–449, 2013, [Online]. Available: http://www.sciencedirect.com/science/article/pii/B9780857095947500107

[86] D. Lesnic, G. Wakefield, B. D. Sleeman, and J. R. Ockendon, “Determination of the index of refraction of anti-reflection coatings,” *Ind. Case Stud. J.*, vol. 2, no. January 2010, pp.

155–173, 2010, [Online]. Available: http://www.micsjournal.ca/index.php/mics/article/view/34

[87] M. R. I. Chowdhury, J. Podder, and A. B. M. O. Islam, “Synthesis and characterization of manganese sulphide thin films deposited by spray pyrolysis,” *Cryst. Res. Technol.*, vol. 46, no. 3, pp. 267–271, 2011, doi: 10.1002/crat.201000549.

[88] P. Chawla, G. Sharma, S. P. Lochab, and N. Singh, “Photoluminescence and optical characterization of CdS nanoparticles prepared by solid-state method at low temperature,” *Radiat. Eff. Defects Solids*, vol. 164, no. 12, pp. 755–762, 2009, doi: 10.1080/10420150903130627.